Persoonia 55, 2025: 203–237
https://www.persoonia.org

RESEARCH ARTICLE

ISSN (Online) 1878-9080
https://doi.org/10.3114/persoonia.2025.55.06

Zombie-ant fungi from western Mexico: six new species in the *Ophiocordyceps unilateralis* complex (*Hypocreales*: *Ascomycota*) and a new host association with *Cephalotes* ants

C.E. Ballesteros-Aguirre[1], T. Sanjuan[2], V. Ramírez-Cruz[1*], A.R. Villalobos-Arámbula[3], M. Vásquez-Bolaños[1], L. Guzmán-Dávalos[1*]

[1]Departamento de Botánica y Zoología, Universidad de Guadalajara, apdo. postal 1–139, Zapopan, Jalisco, 45147, Mexico
[2]Corporación Grupo Micólogos Colombia, Bogotá, Colombia
[3]Departamento de Biología Celular y Molecular, Universidad de Guadalajara, Zapopan, Jalisco, Mexico

*Corresponding authors: L. Guzmán-Dávalos, laura.guzman@academicos.udg.mx; V. Ramírez-Cruz, virginia.ramirez24@academicos.udg.mx

Key words:
ant pathogens
ascospore germination
Camponotini
extended phenotype
funga
Myrmicinae
new taxa

Abstract: The myrmecophilous hirsutelloid fungi of the *Ophiocordyceps unilateralis* complex are common in tropical forests around the world. They are known as zombie-ant fungi because they manipulate the behaviour of ants, since infected ants are forced to move to specific sites in the forest, with optimal environmental conditions for the development of the fungus sporocarp or sporome and the release of the spores. Once there, the ants grab to the substrate with their mandibles, die, and their body becomes a source of nutrients for the fungus. Most of the species of the *O. unilateralis* complex have been described from the Neotropics and the East and Southeast Asia. However, it is likely that there are still many unknown species due to the diversity of their hosts and different specific associations. In this study, we describe six new species of the *O. unilateralis* complex from western Mexico: *O. camponoti-striati*, *O. cephalotiphila*, *O. deltoroi*, *O. haraveriensis*, *O. jaliscana*, and *O. pseudocamponoti-atricipis*, based on morphological characters, phylogenetic analyses of DNA sequences (18S, *TEF1*, *RPB1*, and *RPB2*), and ecological data. We found the following host associations: one fungus – one ant, two fungi – one ant, and one fungus – two ants. Furthermore, we confirmed the host species of the ant genera *Camponotus* and *Colobopsis* (*Formicinae*) based on morphological characters and *COI* sequences, but we also found two species of *Cephalotes* (*Myrmicinae*) susceptible to fungal attack, challenging the paradigm that the *O. unilateralis* complex is a specific parasite of *Camponotini* (*Formicinae*) ants. This study provides insights into the evolution and host range of the *Ophiocordyceps unilateralis* complex in Mexico.

Citation: Ballesteros-Aguirre CE, Sanjuan T, Ramírez-Cruz V, Villalobos-Arámbula AR, Vásquez-Bolaños M, Guzmán-Dávalos L (2025). Zombie-ant fungi from western Mexico: six new species in the *Ophiocordyceps unilateralis* complex (*Hypocreales*: *Ascomycota*) and a new host association with *Cephalotes* ants. *Persoonia* **55**: 203–237. doi: 10.3114/persoonia.2025.55.06
Received: 8 April 2025; **Accepted:** 19 April 2025; **Effectively published online:** 16 September 2025
Corresponding editor: P.W. Crous

INTRODUCTION

Most fungal species of *Ophiocordyceps* (*Hypocreales*: *Ascomycota*) exhibiting manipulative behaviour have been found to be associated with ants. Evolution has allowed some of their fungal genes to express an extended phenotype, in other words, they have effects on the ants' behaviour (Dawkins 1982). When the spores infect and penetrate the ant cuticle, these fungi change into a yeast-like form and excreted metabolites in the middle of the muscle fibres of the ants. These metabolites have the power to induce a specific sequence of behavioural manipulation (Andersen *et al.* 2009, de Bekker *et al.* 2014, 2015, 2017, Araújo *et al.* 2018, Beckerson *et al.* 2023). Ants are forced to die attached with its mandibles to the leaves or other parts of the forest, where there are good environmental conditions for the development of the fungal stromata, which develop directly from the host; for this reason, they were named "zombie-ant fungi" (Andersen *et al.* 2009, Pontoppidan *et al.* 2009, Sanjuan *et al.* 2001, Evans *et al.* 2011, Araújo *et al.* 2020).

The whole ant body becomes a structure for spore dispersal, as well as for protection, a source of nutrients, and to ensure reproductive success (Andersen *et al.* 2009). Many of these manipulative species belong to the clade of hirsutelloid myrmecophilous pathogens, which comprises the *O. unilateralis* complex and the *O. kniphofioides* complex, as well as *O. desmidiospora* and *O. oecophyllae* (Araújo *et al*. 2018, Saltamachia & Araújo 2020). Among them, the *O. unilateralis* complex is the most diverse, associated with ants of the tribe *Camponotini* (*Formicinae*), including the genera *Camponotus*, *Colobopsis*, *Dinomyrmex*, and *Polyrhachis* (Tang *et al*. 2023a, b, c).

The localized places in the environment with high density of dead ants, which were killed by the zombie-ant fungi, were described by de Andrade (1980), Evans & Samson (1982), and Sanjuan *et al.* (2001), and called "graveyards" by

Pontoppidan *et al.* (2009). Zombie-ant fungi are distributed in patches in different sites of the forest, their density being correlated with humidity, temperature, light, and vegetation (Pontoppidan *et al.* 2009, Andriolli *et al*. 2019, Cardoso *et al*. 2019, Lavery *et al.* 2021, Will *et al.* 2022). One of the means of dispersal of these fungi is through ascospores, which are actively discharged from mature specimens in the graveyards (Andersen *et al.* 2009). The ascospores can germinate on the forest floor as a secondary spore, the capilliconidiospore, giving the fungus another chance to infect (Evans *et al.* 2011b, Araújo & Hughes 2016). In addition, the body of the dead ants may be covered with different hirsutelloid asexual morphs that infect, through direct contact, those ants that venture into graveyards (Evans *et al.* 2011a, Araújo & Hughes 2017). Therefore, when the victims of the fungi congregate in graveyards, a kind of "killing fields" are created (Andersen *et al.* 2009).

The site and substrate where the ant bites before dying are variable according to the specific extended phenotype and the environment (Araújo *et al.* 2018). Loreto *et al.* (2018) analysed the correlation between the biting substrate (leaves vs twigs) in two different environments (tropical and temperate) according to the world records of the *O. unilateralis* complex. They suggested that leaf biting is the ancestral condition and twig biting is a derived character, which evolved independently in multiple temperate forests due the availability of stable twigs vs leaves. The twigs last for many seasons; therefore, they are a stable substrate for the fungus to develop. In contrast, the leaves in deciduous trees are lost periodically. The duration of the zombie-ant fungi in the substrate is longer in the temperate forest, specifically on twigs, where the complete development of the fungi occurs in at least one year. However, the most prevalent manipulation observed in the *O. unilateralis* complex is leaf biting (Loreto *et al*. 2018).

In total, 41 species have been described in the *O. unilateralis* complex in temperate and tropical forests of America, Australia, and East and Southeast Asia (Araújo *et al.* 2018, Tang *et al.* 2023a, b, c). It is hypothesized that the origin of this group of entomopathogenic fungi is Southeast Asia (Hywel-Jones 2002, Evans *et al*. 2018, Loreto *et al*. 2018). Nevertheless, it has also been suggested that hundreds of species could exist worldwide due to the diversity of their hosts (Evans *et al.* 2011b, Mackay 2019). The *O. unilateralis* complex is distinguished from other fungi by the presence of a globose to subglobose unilateral perithecial cushion on the stroma, hirsutelloid asexual morphs with generally bottle-shaped conidiogenous cells (phialides), and by its specific association with the ant tribe *Camponotini* (Patouillard 1892, Minter & Brady 1980, Sung *et al.* 2007, Araújo *et al.* 2018). Systematic publications on this complex include those of Tulasne & Tulasne (1865), Schroeter (1894), Saccardo (1895), Petch (1924, 1931, 1934), Kobayasi (1941), Mains (1951, 1958), Evans & Samson (1982, 1984), Sung *et al.* 2007, Evans *et al*. (2011a, b, 2018), Kepler *et al.* (2011), Luangsa-ard *et al.* (2011), Kobmoo *et al.* (2012, 2015, 2019), Araújo *et al*. (2015, 2018), Sanjuan *et al.* (2015), Crous *et al.* (2016), Lin *et al.* (2020), Saltamachia & Araújo (2020), Wei *et al.* (2020), Tang *et al.* (2023a, b, c), and Lu *et al.* (2024).

According to the review by López-Rodríguez *et al*. (2023), there are no records of the *O. unilateralis* complex from Mexico. The purpose of this work was to describe six new species of hirsutelloid myrmecophilous fungi of the *O. unilateralis* complex found in tropical forests in western Jalisco, Mexico, based on molecular phylogeny and morphological, ecological, and distribution data. Furthermore,

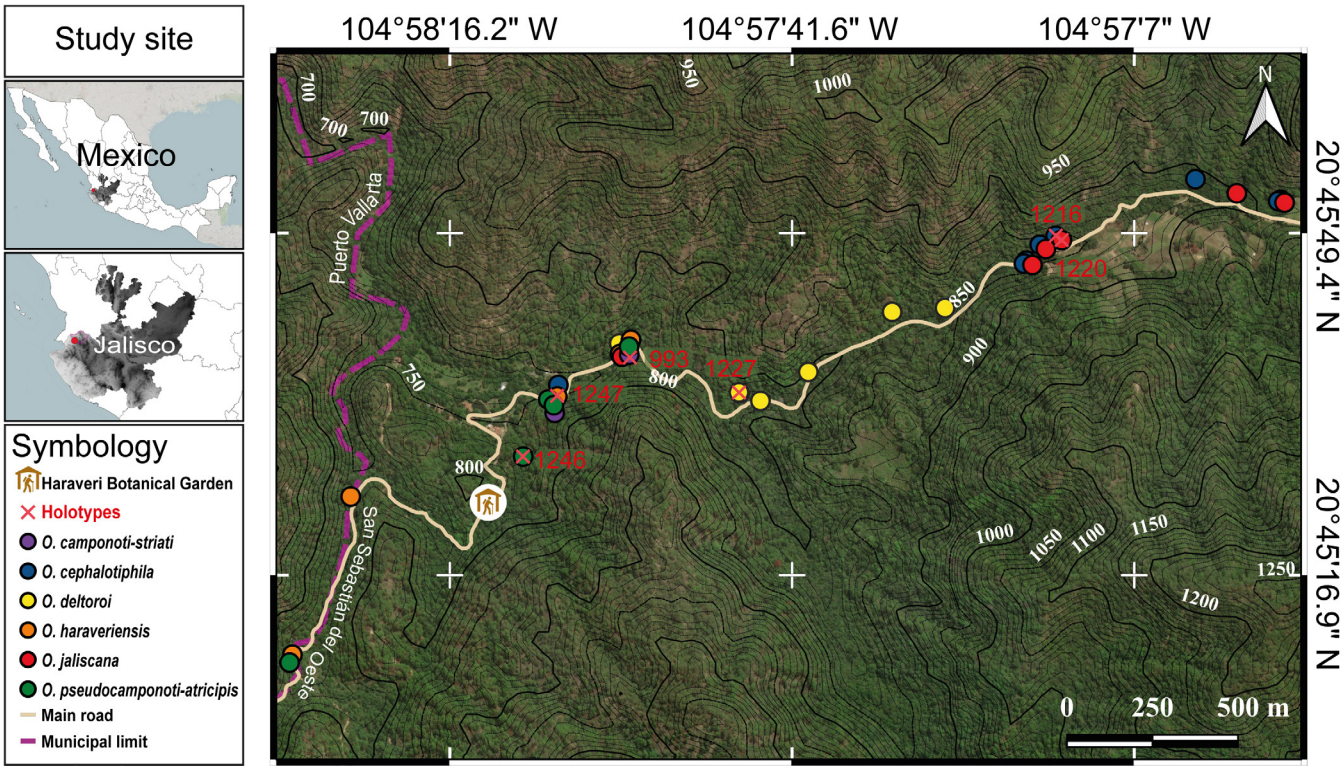

Fig. 1. Distribution of zombie-ant graveyards in the study location, in tropical forests surrounding and into the Haravéri Botanical Garden, close to the village La Estancia de Landeros, municipality of San Sebastián del Oeste, Jalisco state, western Mexico. Each colour means a different species of *Ophiocordyceps*. The holotypes are marked with a red cross and the specimen number of C.E. Ballesteros-Aguirre in red.

the evolutionary relationships of the Mexican members of *O. unilateralis* complex and its host are discussed here.

MATERIAL AND METHODS

Sampling

The sampling was carried out in tropical forests surrounding and into the Haravéri Botanical Garden, inside of the buffer area in the biosphere reserve Sierra de Vallejo-Río Ameca (CONANP 2023), municipality of San Sebastián del Oeste, Jalisco state, western Mexico. We sampled during the dry and rainy seasons in intervals of 45 d approximately, from December 2020 to October 2021. A survey of zombie-ant graveyards (epizootics) was carried out in three types of forests: tropical montane cloud forest (TMCF), gallery forest (GF), and subdeciduous tropical forest (SDTF), according to the classification of Rzedowski (2006) (Fig. 1). We sampled in detail the different substrates where the ants die: leaves, stems, twigs, branches, trunks, base of plants, and base of rocks, from the ground up to 3 m high. The distance between the closest and the furthest zombie-ant fungus to the forest floor was recorded in each graveyard.

For each of the six morphotypes of the *O. unilateralis* complex, 2 to 10 zombie-ant graveyards were selected; in total, 37 graveyards were sampled. The collection of several individuals of zombie-ant fungi, of a certain species in each graveyard, and collected on the same date was considered a specimen, according to article 8.2 of Shenzhen code (Turland *et al.* 2018). Specimens were photographed in situ with an electronic tablet, a digital EOS R7 Canon camera, macro lens, and led lamps. Multiple individuals of each specimen were selected for DNA extraction, microscopy study, and ascospore germination. To obtain mature ascospores and germinate them, the most vigorous specimens with perithecial cushions in each morphotype were separated and kept in previously sterilized humid chambers, held in place with Vaseline on top of a slide, inside Falcon® tubes [instead of plastic Petri dishes with distilled water agar or potato dextrose agar (PDA)], modified from Araújo *et al*. (2018). The humid chambers were secured inside a plastic shipping container and checked one week later. The specimens were deposited in the collection of fungi of the IBUG Fungarium of the Instituto de Botánica, Universidad de Guadalajara, Zapopan, Jalisco, Mexico (Table S1 https://doi.org/10.6084/m9.figshare.29094056). Additionally, apparently healthy ants were collected in each graveyard and preserved in 96 % undenatured ethyl alcohol (Table S2 https://doi.org/10.6084/m9.figshare.29094056).

Morphological studies

Macromorphological characters of both fungi and hosts were examined under a dissecting microscope (Carl Zeiss Stemi SV6, Germany) and micromorphological characters of fungi in an optical microscope (Carl Zeiss Axio Scope, Germany). ZEN v. 2.3 software was employed for taking measurements and photographs. The photographs were processed with CombineZP software for an extended depth of field (Hadley 2010, Brecko *et al.* 2014), and edited in Adobe Illustrator®. Fungi were cut freehand with razor blades and tweezers, hydrated with water or 70 % ethyl alcohol, and mounted on slides in 3 % KOH (Guzmán *et al*. 2001), or stained with Congo red (Steensma 2001). The slides were observed in the optical microscope to make the descriptions of the characteristics of the mycelia, stromata, perithecial cushions, perithecia (= ascomata), asci, ascospores, capilliconidiophores, capilliconidia, phialides, and conidia (Evans & Samson 1982, 1984, Araújo *et al.* 2018). For the descriptions of the asexual morphs, we followed the *Hirsutella* types described by Evans *et al.* (2011a), specifically A and C (Fig. 2F, G).

A careful inspection of the slides of the humid chambers was carried out 1 wk after the specimens were obtained in the field; the presence of mature ascospores, capilliconidiophores, capilliconidia, or mycelium was reported. The positive samples were fixed with lactophenol (Maneval 1936) and deposited in the collection of fungi at IBUG. For the morphological comparison with other species of the *O. unilateralis* complex, 30–50 measurements were made in each mentioned taxonomic character (Table S1).

Non-parasitized ants were mounted on entomological pins and deposited in the entomological collection CZUG of the Centro de Estudios en Zoología, Universidad de Guadalajara (Fig. 2, Table S2). The following were consulted for their determination: Pergande (1896), Wheeler (1931), Mackay & Mackay (1989, 2018), de Andrade & Baroni Urbani (1999), Palacio & Fernández (2003), Vásquez-Bolaños (2011, 2015), Mackay (2019), AntCat (Bolton 2024), AntMaps (Janicki *et al*. 2016, Guénard *et al.* 2017), AntWeb (2023), and AntWiki (2023).

DNA extraction, PCR, and sequencing

All samples were collected in their natural environment. For DNA extraction, samples of stroma and the fungal pseudosclerotium from inside the gaster of the parasitized ants were obtained in the laboratory by dissecting the ant's abdomen; the fungi were cut with a new razor blade and the help of tweezers under stereoscopic microscope to avoid the presence of contaminants (e.g., other fungi, lichens or mosses). The samples were frozen in an ultra-freezer at approximately -70 °C and pulverized with metallic spheres in a TissueLyser II (Qiagen, Germany). Total genomic DNA was extracted using a modified salt-extraction method with 1 % PVP (Aljanabi & Martinez 1997). Four loci were amplified through PCR reactions: small subunit of the nuclear ribosomal DNA (18S), translation elongation factor 1-α (*TEF1*), and the largest and second largest subunits of RNA polymerase II (*RPB1* & *RPB2*). The primer pairs used were for 18S: NS1/NS4 (White *et al.* 1990), *TEF1*: 983F/2218R, *RPB1*: CRPB1/RPB1Cr_oph (Castlebury *et al.* 2004, Araújo *et al.* 2018), and for *RPB2*: fRPB2–5f/fRPB2–7cR (Liu *et al.* 1999). Each 54.15 µL amplification reaction contained 35 µL of PCR-grade water, 6 µL of 10× *Taq* reaction buffer without MgCl2, 3 µL of 50 mM MgCl2, 3 µL of 5 mM dNTP, and 3 µL of 2 µg/µL Bovine Serum Albumine, then 1 µL of each 10 mM primer, 2 µL of DNA template, and 0.15 µL Platinum™ *Taq* DNA Polymerase High Fidelity (5 U/µL) were added. End concentrations of the PCR reagents were 1.1× *Taq* reaction buffer without MgCl2, 2.7 mM MgCl2, 0.3 mM dNTP's, 0.1 µg/µL BSA, 0.18 µM of each primer, and 0.01 U/µL *Taq* DNA Polymerase. A Swift MaxPro thermocycler (Esco) was used under the following PCR conditions for each region: 94 °C for 3 min, 35 cycles at

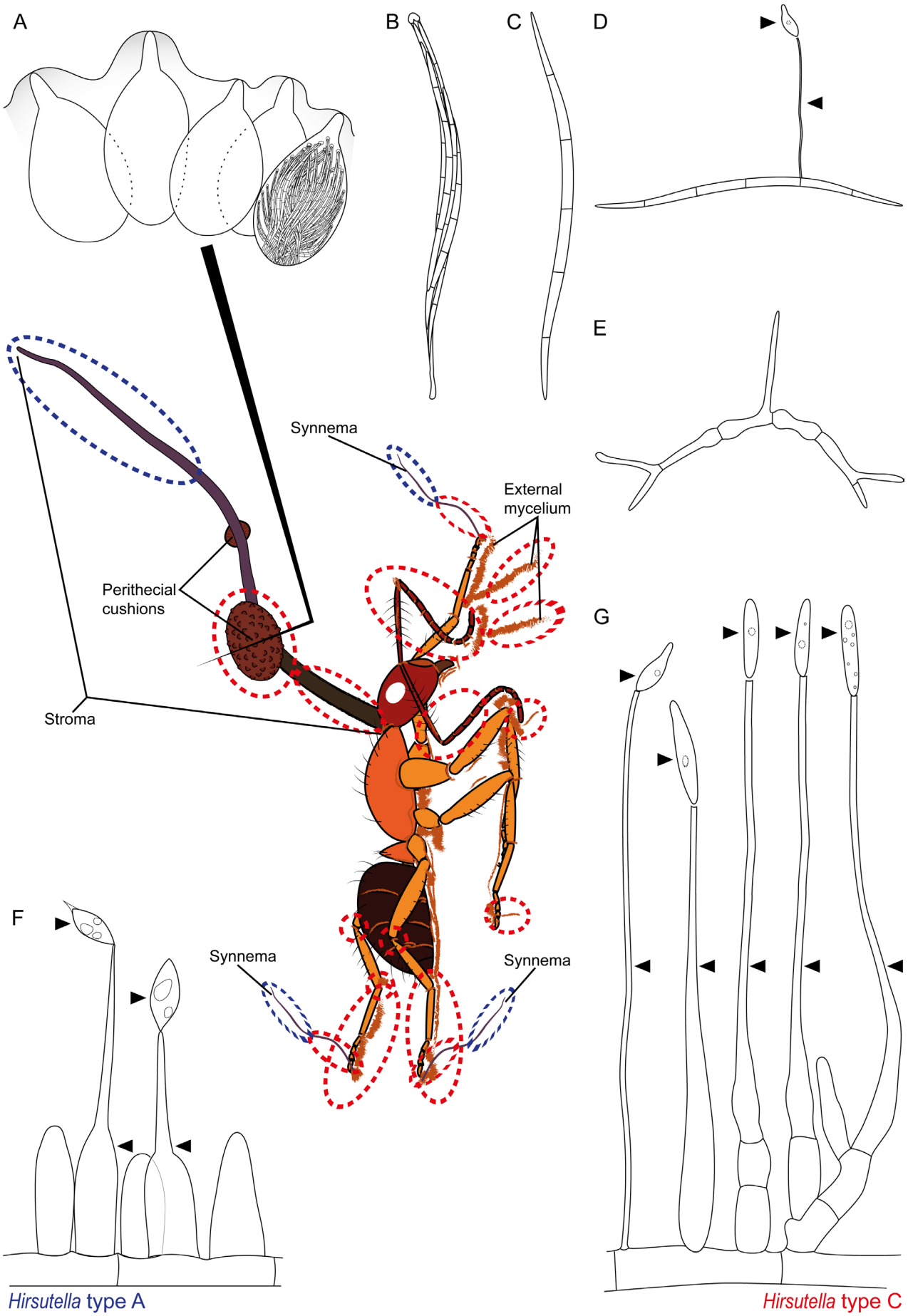

Fig. 2. Structures considered here in the microscopic study of *Ophiocordyceps unilateralis* complex. **A.** Perithecia (= ascomata). **B.** Ascus. **C.** Ascospore. **D.** Germinated ascospore in capilliconidiophore (left arrow) and capilliconidium (right arrow). **E.** Germinated ascospore in somatic hyphae. **F.** *Hirsutella* type A present in the stromal apex and in the synnemata (blue dotted line), phialides (left arrow) and conidia (right arrow). **G.** *Hirsutella* type C present on stromal base, different parts of the ant, the surface of perithecial cushions, and the external mycelium that adheres the ant to the substrate (red dotted line), phialides (left arrow) and conidia (right arrow).

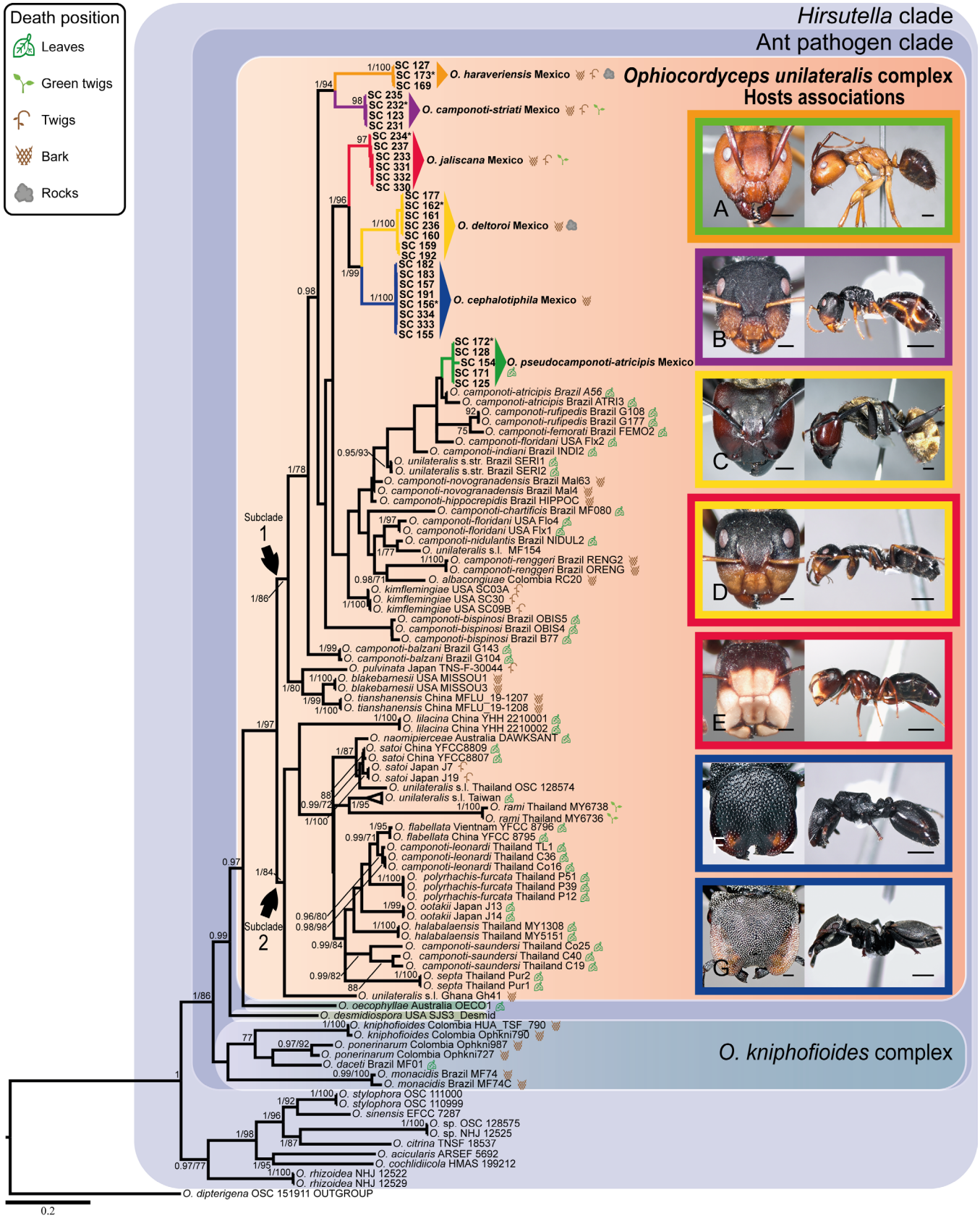

Fig. 3. Phylogenetic relationships of the *Ophiocordyceps unilateralis* complex and other species of *Ophiocordyceps* based on 18S, *TEF1*, *RPB1*, and *RBP2*. The topology from ML analyses is shown. The bar indicates the rate of nucleotide substitution. The support values correspond to BI and ML analyses. Only PP ≥ 0.95 and maximum likelihood BS ≥ 70 % are shown. Sequences generated in this work are in **bold**. Holotypes are indicated by an asterisk. The death positions of ants (extended phenotype of the fungi) are marked with symbols. Each colour in the clades and ant boxes means a different species of *Ophiocordyceps*: *O. camponoti-striati*, purple; *O. cephalotiphila*, blue; *O. deltoroi*, yellow; *O. haraveriensis*, orange; *O. jaliscana*, red; *O. pseudocamponoti-atricipis*, green. Major workers (soldiers) of associated hosts: **A.** *Camponotus* sp. 4 (*Camp. atriceps* s. l.). **B.** *Camponotus* sp. 1 (*Camp. striatus* s. l.). **C.** *Camponotus* sp. 2 (*Camp. sericeiventris* s. l.). **D.** *Camponotus* sp. 3 (*Camp. tepicanus* s. l.). **E.** *Colobopsis* sp. **F.** *Cephalotes hirsutus*. **G.** *Cephalotes goniodontus.* Scale bars in ant heads: A, C = 1 mm; B, D–G = 250 µm; in ant lateral views: A–G = 1 mm.

94 °C for 30 s, 55 °C (*18S* and *RPB2*), 52 °C (*TEF1*), or 47 °C (*RPB1*) for 1 min, 72 °C for 2 min, and a final extension at 72 °C for 10 min. The PCR products were separated by electrophoresis in 1.5 % agarose gels with GelRed Nucleid Acid Stain 10000× (Biotium, USA) in water and visualized in an Amersham Imager 600 (General Electric Company, USA). The PCR products were purified with GFX columns (Qiagen, Germany) or with ExoSAP-IT (Applied Biosystem, Lithuania), following the protocol recommended by the fabricant. We performed Sanger sequencing at the University of Arizona Genetics Core. The DNA sequences were visualized and manually edited, when necessary, in ChromasPro v. 2.1.10 (Technelysium 1996). To ensure that the sequences of fungi and ants belong to the corresponding genus, BLAST® was employed (Altschul *et al.* 1990). The new sequences were deposited in NCBIs GenBank nucleotide database (Sayers *et al.* 2022), and accession numbers are indicated in Table 1.

Phylogenetic analyses

We constructed four matrices with DNA sequences, one for each locus (18S, *TEF1*, *RPB1*, and *RPB2*), from the species of the *O. unilateralis* complex and related hirsutelloid fungi (*Hirsutella* clade based on Tang *et al.* 2023a). Sequences not generated in this study were obtained from GenBank (Table 1). *Ophiocordyceps dipterigena* was selected as outgroup (Tang *et al.* 2023a). Each matrix was analysed separately with Maximum Likelihood (ML) to test for strongly supported gene conflict and then, if there was no conflict, all of them were concatenated into a single super matrix. The matrices were constructed in PhyDE® v. 0.9971 (Müller *et al.* 2005) and aligned with MUSCLE v. 3.8.31 (Edgar 2004). The final alignment included 139 taxa and 3816 positions after removing ambiguous positions, due to insertions or deletions, and the beginning and end of the alignment. The reading frame was adjusted manually. Concatenated dataset consisted of 10 data partitions: one for 18S (1026 bp) and three for each of the codon positions (1st, 2nd, and 3rd) of the three protein-coding genes: *TEF1* (1028 bp), *RPB1* (668 bp, without the intron that was removed), and *RPB2* (1091 bp). The phylogenetic inference analyses were performed with computational resources from CIPRES (Miller *et al.* 2010). The ML analyses were performed in RAxML v. 8.2.12 (Stamatakis 2014) on XSEDE (Towns *et al.* 2014), with the GTRGAMMA+I model of nucleotide substitutions and 1000 bootstrap replicates (BS). Bayesian inference (BI) analyses were performed with MrBayes v. 3.2.2 (Ronquist *et al.* 2012) on XSEDE with GTRGAMMA+I model. Two independent runs of 10 M generations were made, which were sampled every 1000, and 25 % of the trees generated were discarded. The remaining trees were used to create a consensus tree. Convergence of Markov Chains Monte Carlo (MCMC) was evaluated by analysing the effective sample size in Tracer v. 1.7.2 (Rambaut *et al.* 2018). Only branches with ≥ 70 % of BS support and posterior probabilities (PP) ≥ 0.95 were considered significant, according to Leaché & Reeder (2002). The trees were visualized in FigTree v. 1.4.4 (Rambaut 2018) and edited with Adobe Illustrator®. Alignments were submitted to Figshare (https://doi.org/10.6084/m9.figshare.29094056).

In the phylogenetic tree (Fig. 3), the extended phenotype of the fungi (i.e., the place where the ants die) is also indicated for each species. This information was taken from the literature or from direct observations on the species described here. We use the following classification: “leaves” when ants die biting the leaves of any kind of plant, “green twigs” on non-woody plants, “twigs” on the bark on twigs, “bark” when they die biting the base or trunk of trees, inside logs, or even on bark cover with lichens or mosses, and “rocks” if the ants die directly at the base of rocks.

RESULTS

Phylogenetic relationships

The topologies of the phylogenetic trees were similar in BI and ML analyses; Fig. 3 shows ML topology. The ant pathogenic clade was well-supported (PP = 1, BS = 86 %); the *Ophiocordyceps kniphofioides* complex formed a distinct but unsupported lineage, and *O. desmidiospora* and *O. oecophyllae* are early-diverging lineages relative to the *O. unilateralis* complex. The *O. unilateralis* complex was recovered with good support (PP = 1, BS = 97 %), and two major subclades were recovered within it: subclade 1 (PP = 1, BS = 86 %) formed with mostly American species, and subclade 2 (PP = 1, BS = 84 %), with mostly Asian species. Phylogenetic analyses showed six distinct clades clustered in subclade 1, corresponding to six new taxa, separated from other American species; three of them with high statistical support (PP = 1, BS = 100 %), two only supported with BS (97 or 98 %), and one without support, which is the case of the *O. pseudocamponoti-atricipis* clade. The latter species was found to be a sister species of *O. camponoti-atricipis*, but this relationship was also not supported.

Regarding the extended phenotype, in subclade 1, most ants died on leaves or bark. In the case of the Mexican species, almost all were found on bark, although *O. camponoti-striati*, *O. haraveriensis*, and *O. jaliscana* also died on twigs. Interestingly, *O. deltoroi* and *O. haraveriensis* also manipulate ants to die on the base of rocks. On the other hand, *O. pseudocamponoti-atricipis* was only found on leaves. Death position on twigs is the ancestral character state of subclade 1, since *O. pulvinata* has a basal position. The subclade 2 showed bark as the ancestral character state according to the position of *O. unilateralis* s. l. from Ghana (Gh41), but in most Asian species, ants prefer to die biting leaves. The extended phenotype when ants die biting the bark is the ancestral state of the hirsutelloid ant pathogen clade.

Taxonomy

Ophiocordyceps camponoti-striati C.E. Ballesteros-Aguirre, T. Sanjuan & L. Guzmán-Dávalos, ***sp. nov.*** MB 859556. Fig. 4.

Etymology: The specific epithet refers to the scientific name of the host ant species *Camponotus striatus*.

Typus: **Mexico**, west of Jalisco state, nearby Haravéri Botanical Garden, 20°45’38.6”N, 104°57’58”W, 766 m.a.s.l., gallery forest, host *Camponotus striatus* s. l. (*Formicinae*: *Camponotini*), minor and major workers (ants’ castes), ants die biting twigs or branches of bushes or trees, on the

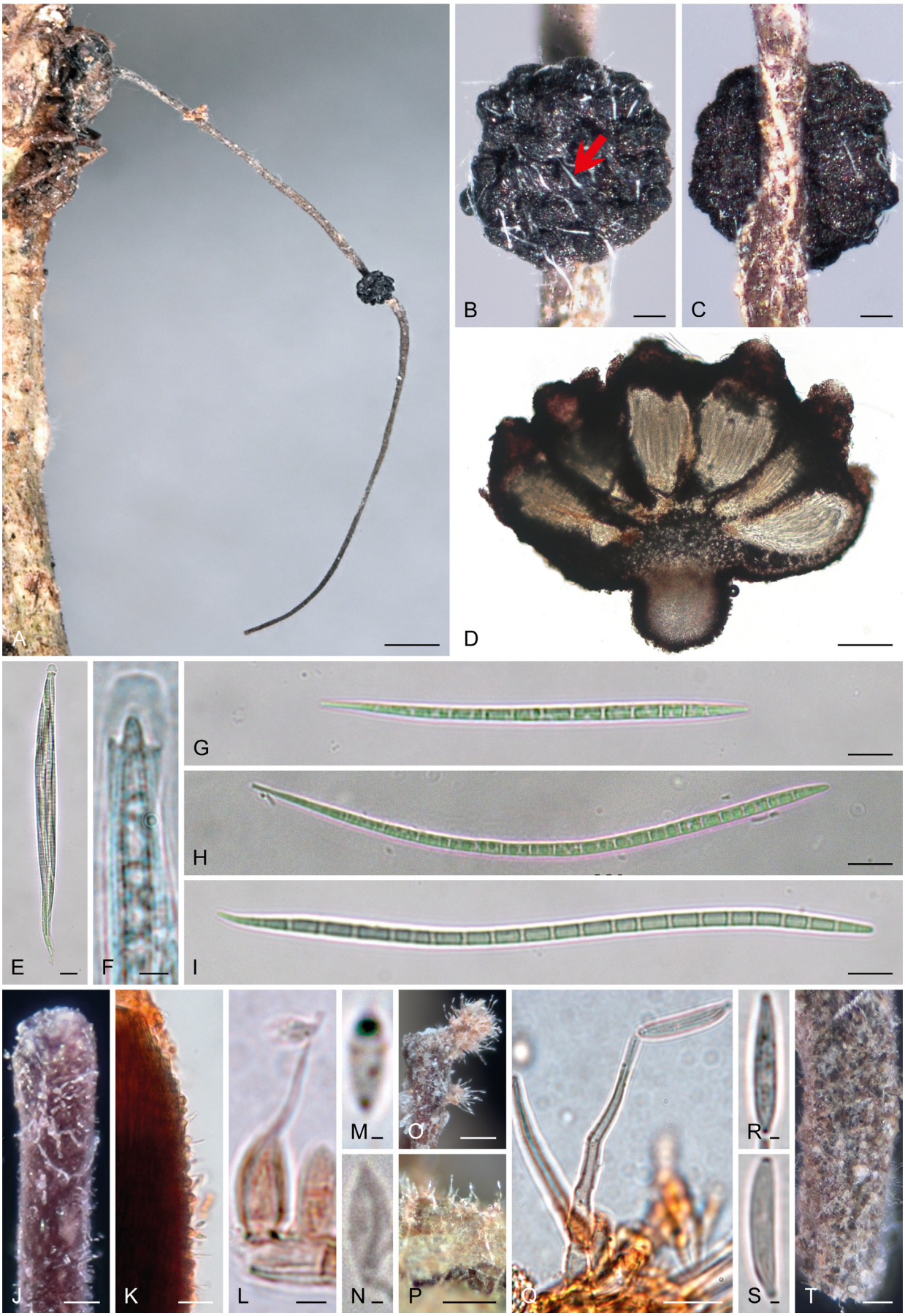

Fig. 4. *Ophiocordyceps camponoti-striati* (A–G, I–M, O–T: C.E. Ballesteros-Aguirre 993 (SC232), holotype; H: C.E. Ballesteros-Aguirre 1132; N: C.E. Ballesteros-Aguirre 145). **A.** Host *Camponotus* sp. 1 (*Camp. striatus* s. l.) biting the bark of a twig with a stroma emerging between the pronotum and head, with a perithecial cushion. **B, C.** Unilaterally attached perithecial cushion produced from the stroma, with ascospores released (red arrow). **D.** Cross-section of the perithecial cushion showing the perithecial arrangement. **E.** Ascus. **F.** Apical region of the ascus. **G–I.** Ascospores with 12−21 septa. **J–N.** Asexual morph *Hirsutella* type A. **J.** Stroma's apex. **K, L.** Phialides. **M, N.** Conidia. **O–S.** Asexual morph *Hirsutella* type C. **O.** Sporodochia upon the ant's antenna. **P.** Phialides from the external mycelium. **Q.** Phialide with a conidium. **R, S.** Conidia. **T.** Base of the stroma. Scale bars: A = 1 mm; B−D, O, P = 100 µm; J, T = 50 µm; E, G, H, I, K, Q = 10 µm; F, L = 2.5 µm; R, S = 1 µm; M, N = 0.5 µm.

Table 1. GenBank accession numbers and specimen information of the sequences of *Ophiocordyceps* used in this study. Sequences generated in this work in **bold**. An asterisk indicates the holotype for the novel species described here.

Current species	Voucher	18S	*TEF1*	*RPB1*	*RPB2*	Host species	Country	Reference
O. acicularis	ARSEF 5692	DQ522540	DQ522322	DQ522368	DQ522418	*Coleoptera*	Korea	Spatafora *et al.* (2007)
O. albacongiuae	RC20	KX713633	KX713670	—	—	*Camponotus* sp.	Colombia	Araújo *et al.* (2018)
O. blakebarnesii	MISSOU1	KX713644	KX713686	KX713713	—	*Camponotus* sp.	USA	Araújo *et al.* (2018)
	MISSOU3	KX713643	KX713687	KX713714	—	*Camponotus* sp.	USA	Araújo *et al.* (2018)
O. camponoti-atricipis	ATRI3	KX713666	KX713677	—	—	*Camponotus atriceps*	Brazil	Araújo *et al.* (2018)
	A56	KJ953886	—	—	—	*Camponotus atriceps*	Brazil	Araújo *et al.* (2015)
O. camponoti-balzani	G104	KX713660	KX713689	KX713703	—	*Camponotus balzani*	Brazil	Araújo *et al.*. (2018)
	G143	KX713658	KX713690	KX713705	—	*Camponotus balzani*	Brazil	Araújo *et al.* (2018)
O. camponoti-bispinosi	B77	KJ953887	—	—	—	*Camponotus bispinosus*	Brazil	Araújo *et al.* (2015)
	OBIS4	KX713637	KX713692	KX713720	—	*Camponotus bispinosus*	Brazil	Araújo *et al.* (2018)
	OBIS5	KX713636	KX713693	KX713721	—	*Camponotus bispinosus*	Brazil	Araújo *et al.* (2018)
O. camponoti-chartificis	MF080	MK874744	MK863824	—	—	*Camponotus chartifex*	Brazil	Araújo *et al.* (2018)
O. camponoti-femorati	FEMO2	KX713663	KX713678	KX713702	—	*Camponotus femoratus*	Brazil	Araújo *et al.* (2018)
O. camponoti-floridani	Flo4	KX713662	—	—	—	*Camponotus floridanus*	USA	Araújo *et al.* (2018)
	Flx1	KX713661	—	—	—	*Camponotus floridanus*	USA	Araújo *et al.* (2018)
	Flx2	—	KX713674	—	—	*Camponotus floridanus*	USA	Araújo *et al.* (2018)
O. camponoti-hippocrepidis	HIPPOC	KX713655	KX713673	KX713707	—	*Camponotus hippocrepis*	Brazil	Araújo *et al.* (2018)
O. camponoti-indiani	INDI2	KX713654	—	—	—	*Camponotus indianus*	Brazil	Araújo *et al.* (2018)
O. camponoti-leonardi	C36/Co24	KJ201512	JN819013	—	—	*Colobopsis leonardi*	Thailand	Kobmoo *et al.* (2012, 2015)
	Co16	—	JN819019	—	—	*Colobopsis leonardi*	Thailand	Kobmoo *et al.* (2012)
	TL1	KJ201515	KJ201526	—	—	*Colobopsis leonardi*	Thailand	Kobmoo *et al.* (2012, 2015)
O. camponoti-nidulantis	NIDUL2	KX713640	KX713669	KX713717	—	*Camponotus nidulans*	Brazil	Araújo *et al.* (2018)
O. camponoti-novogranadensis	Mal63	KX713648	—	—	—	*Camponotus novogranadensis*	Brazil	Araújo *et al.* (2018)
	Mal4	KX713649	—	—	—	*Camponotus novogranadensis*	Brazil	Araújo *et al.* (2018)
O. camponoti-renggeri	ORENG	KX713634	KX713671	—	—	*Camponotus renggeri*	Brazil	Araújo *et al.* (2018)
	RENG2	KX713632	KX713672	—	—	*Camponotus renggeri*	Brazil	Araújo *et al.* (2018)
O. camponoti-rufipedis	G108	KX713659	KX713679	KX713704	—	*Camponotus rufipes*	Brazil	Araújo *et al.* (2018)
	G177	KX713657	KX713680	—	—	*Camponotus rufipes*	Brazil	Araújo *et al.* (2018)
O. camponoti-saundersi	Co25	—	JN819012	—	—	*Colobopsis saundersi*	Thailand	Kobmoo *et al.* (2012)
	C40	KJ201519	—	—	—	*Colobopsis saundersi*	Thailand	Kobmoo *et al.* (2012)
	C19/Co22	KJ201520	JN819015	—	—	*Colobopsis saundersi*	Thailand	Kobmoo *et al.* (2012, 2015)
O. camponoti-striati	**SC123**	**PV745526**	**PV759173**	**PV759210**	—	***Camponotus striatus* s. l.**	**Mexico**	**This study**
	SC231	**PV745527**	—	—	—	***Camponotus striatus* s. l.**	**Mexico**	**This study**

Table 1. (Continued).

Current species	Voucher	18S	*TEF1*	*RPB1*	*RPB2*	Host species	Country	Reference
	SC232*	**PV745528**	**PV759174**	**PV759211**	—	***Camponotus striatus* s. l.**	**Mexico**	**This study**
	SC235	**PV745529**	**PV759175**	—	—	***Camponotus striatus* s. l.**	**Mexico**	**This study**
O. cephalotiphila	**SC155**	—	—	**PV759212**	**PV759196**	***Cephalotes goniodontus***	**Mexico**	**This study**
	SC157	—	—	**PV759213**	—	***Cephalotes goniodontus***	**Mexico**	**This study**
	SC183	—	—	**PV759214**	—	***Cephalotes goniodontus***	**Mexico**	**This study**
	SC333	**PV745530**	—	—	—	***Cephalotes goniodontus***	**Mexico**	**This study**
	SC334	**PV745531**	—	—	—	***Cephalotes goniodontus***	**Mexico**	**This study**
	SC156*	**PV745532**	**PV759176**	**PV759215**	**PV759197**	***Cephalotes hirsutus***	**Mexico**	**This study**
	SC182	**PV745533**	**PV759177**	—	**PV759198**	***Cephalotes hirsutus***	**Mexico**	**This study**
	SC191	**PV745534**	**PV759178**	**PV759216**	**PV759199**	***Cephalotes hirsutus***	**Mexico**	**This study**
O. citrina	TNSF 18537	—	KJ878983	—	KJ878954	*Hemiptera*	Japan	Quandt *et al.* (2014)
O. cochlidiicola	HMAS 199212	KJ878917	KJ878965	KJ878998	—	*Lepidoptera*	China	Quandt *et al.* (2014)
O. daceti	MF01	—	KX713667	—	—	*Daceton armigerum*	Brazil	Araújo *et al.* (2018)
O. deltoroi	**SC159**	—	**PV759179**	**PV759217**	—	***Camponotus sericeiventris* s. l.**	**Mexico**	**This study**
	SC160	**PV745535**	**PV759180**	**PV759218**	**PV759200**	***Camponotus sericeiventris* s. l.**	**Mexico**	**This study**
	SC161	**PV745536**	**PV759181**	**PV759219**	**PV759201**	***Camponotus sericeiventris* s. l.**	**Mexico**	**This study**
	SC162*	**PV745537**	**PV759182**	**PV759220**	—	***Camponotus sericeiventris* s. l.**	**Mexico**	**This study**
	SC177	—	**PV759183**	**PV759221**	—	***Camponotus sericeiventris* s. l.**	**Mexico**	**This study**
	SC192	**PV745538**	**PV759184**	**PV759222**	**PV759202**	***Camponotus tepicanus***	**Mexico**	**This study**
	SC236	**PV745539**	**PV759185**	**PV759223**	**PV759203**	***Camponotus tepicanus***	**Mexico**	**This study**
O. desmidiospora	SJS3_Desmid	MH536515	MN785129	MN785131	—	*Camponotus pennsylvanicus*	USA	Saltamachia & Araújo (2020)
O. dipterigena	OSC 151911	KJ878919	KJ878966	KJ879000	—	*Diptera*	USA	Quandt *et al.* (2014)
O. flabellata	YFCC 8795	OL310721	OL322688	OL322687	OL322695	*Camponotus* sp.	China	Tang *et al.* (2023a)
	YFCC 8796	OL310722	OL322692	OL322689	OL322696	*Camponotus* sp.	Vietnam	Tang *et al.* (2023a)
O. halabalaensis	MY5151	KM655826	GU797110	—	—	*Dinomyrmex gigas*	Thailand	Luangsa-ard *et al.* (2011), Kobmoo *et al.* (2015)
	MY1308	KM655825	GU797109	—	—	*Dinomyrmex gigas*	Thailand	Luangsa-ard *et al.* (2011), Kobmoo *et al.* (2015)
O. haraveriensis	**SC127**	**PV745540**	**PV759186**	**PV759224**	**PV759204**	***Camponotus atriceps* s. l.**	**Mexico**	**This study**
	SC169	**PV745541**	**PV759187**	**PV759225**	—	***Camponotus atriceps* s. l.**	**Mexico**	**This study**
	SC173*	**PV745542**	**PV759188**	—	—	***Camponotus atriceps* s. l.**	**Mexico**	**This study**
O. jaliscana	**SC233**	**PV745543**	**PV759189**	**PV759226**	**PV759205**	***Colobopsis* sp.**	**Mexico**	**This study**
	SC234*	**PV745544**	**PV759190**	**PV759227**	**PV759206**	***Colobopsis* sp.**	**Mexico**	**This study**
	SC237	**PV745545**	**PV759191**	**PV759228**	**PV759207**	***Camponotus tepicanus***	**Mexico**	**This study**
	SC330	**PV745546**	—	—	—	***Camponotus tepicanus***	**Mexico**	**This study**

Table 1. (Continued).

Current species	Voucher	18S	*TEF1*	*RPB1*	*RPB2*	Host species	Country	Reference
	SC331	**PV745547**	—	—	—	***Camponotus tepicanus***	**Mexico**	**This study**
	SC332	**PV745548**	—	—	—	***Camponotus tepicanus***	**Mexico**	**This study**
O. kimflemingiae	SC09B	KX713631	KX713698	KX713724	—	*Camponotus castaneus / americanus*	USA	Araújo *et al.* (2018)
	SC30	KX713629	KX713699	KX713727	—	*Camponotus castaneus / americanus*	USA	Araújo *et al.* (2018)
	SC03A	—	KX713697	KX713722	—	*Camponotus castaneus / americanus*	USA	Araújo *et al.* (2018)
O. kniphofioides	HUA_TSF_790	MF416620	MF416513	MF416670	—	*Cephalotes atratus*	Colombia	Kepler *et al.* (2017)
	Ophkni790	KC610789	KC610740	KF658668	—	*Cephalotes atratus*	Colombia	Sanjuan *et al.* (2015)
O. lilacina	YHH 2210001	OP782343	OP796856	OP796861	—	*Polyrhachis* sp.	China	Tang *et al.* (2023a)
	YHH 2210002	OP782344	OP796857	OP796862	—	*Polyrhachis* sp.	China	Tang *et al.* (2023a)
O. monacidis	MF74	KX713647	—	KX713712	—	*Dolichoderus bispinosus*	Brazil	Araújo *et al.* (2018)
	MF74C	KX713646	—	—	—	*Dolichoderus bispinosus*	Brazil	Araújo *et al.* (2018)
O. naomipierceae	DAWKSANT	KX713664	—	KX713701	—	*Polyrhachis* sp.	Australia	Araújo *et al.* (2018)
O. oecophyllae	OECO1	KX713635	—	—	—	*Oecophylla smaragdina*	Australia	Araújo *et al.* (2018)
O. ootakii	J13	KX713652	KX713681	KX713708	—	*Polyrhachis moesta*	Japan	Araújo *et al.* (2018)
	J14	KX713651	KX713682	KX713709	—	*Polyrhachis moesta*	Japan	Araújo *et al.* (2018)
O. polyrhachis-furcata	P39/Po21	KJ201504	JN819003	—	—	*Polyrhachis furcata*	Thailand	Kobmoo *et al.* (2012, 2015)
	P51/Po24	KJ201505	JN819000	—	—	*Polyrhachis furcata*	Thailand	Kobmoo *et al.* (2012, 2015)
	P12/Po26_1	KJ201506	JN819030	—	—	*Polyrhachis furcata*	Thailand	Kobmoo *et al.* (2012, 2015)
O. ponerinarum	Ophkni727	KC610790	KC610739	KF658667	KC610717	*Paraponera clavata*	Colombia	Sanjuan *et al.* (2015)
	Ophkni987	—	—	KF658669	n/a	*Paraponera clavata*	Colombia	Sanjuan *et al.* (2015)
O. pseudocamponoti-atricipis	**SC125**	**PV745549**	—	—	—	***Camponotus atriceps* s. l.**	**Mexico**	**This study**
	SC128	**PV745550**	**PV759192**	—	—	***Camponotus atriceps* s. l.**	**Mexico**	**This study**
	SC154	**PV745551**	**PV759193**	**PV759229**	**PV759208**	***Camponotus atriceps* s. l.**	**Mexico**	**This study**
	SC171	**PV745552**	**PV759194**	—	—	***Camponotus atriceps* s. l.**	**Mexico**	**This study**
	SC172*	**PV745553**	**PV759195**	—	**PV759209**	***Camponotus atriceps* s. l.**	**Mexico**	**This study**
O. pulvinata	TNS-F-30044	GU904208	GU904209	GU904210	—	*Camponotus obscuripes*	Japan	Kepler *et al.* (2017)
O. rami	MY6738	KM655824	KJ201534	—	—	*Camponotus* sp.	Thailand	Kobmoo *et al.* (2015)
	MY6736	KM655823	KJ201532	—	—	*Camponotus* sp.	Thailand	Kobmoo *et al.* (2015)
O. rhizoidea	NHJ 12529	EF468969	EF468765	EF468872	EF468922	*Coleoptera*	—	Sung *et al.* (2007)
	NHJ 12522	EF468970	EF468764	EF468873	EF468923	*Coleoptera*	—	Sung *et al.* (2007)
O. satoi	J7	KX713653	KX713683	KX713711	—	*Polyrhachis lamellidens*	Japan	Araújo *et al.* (2018)
	J19	KX713650	KX713684	KX713710	—	*Polyrhachis lamellidens*	Japan	Araújo *et al.* (2018)
	YFCC 8807	OP782340	OP796853	OP796858	OP796863	*Polyrhachis* sp.	China	Tang *et al.* (2023a)
	YFCC 8809	OP782341	OP796854	OP796859	OP796864	*Polyrhachis* sp.	China	Tang *et al.* (2023a)

Table 1. (Continued).

Current species	Voucher	18S	*TEF1*	*RPB1*	*RPB2*	Host species	Country	Reference
O. septa	Pur1	—	KJ201528	—	—	*Camponotus* sp.	Thailand	Kobmoo *et al.* (2015)
	Pur2	—	KJ201529	—	—	*Camponotus* sp.	Thailand	Kobmoo *et al.* (2015)
O. sinensis	EFCC 7287	EF468971	EF468767	EF468874	EF468924	*Lepidoptera*	—	Sung *et al.* (2007)
O. stylophora	OSC 111000	DQ522552	DQ522337	DQ522382	DQ522433	*Coleoptera*	—	Spatafora *et al.* (2007)
	OSC 110999	EF468982	EF468777	EF468882	EF468931	*Coleoptera*	—	Sung *et al.* (2007)
O. tianshanensis	MFLU 19-1207	MN025409	MK992784	—	—	*Camponotus japonicus*	China	Wei *et al.* (2020)
	MFLU 19-1208	MN025410	MK992785	—	—	*Camponotus japonicus*	China	Wei *et al.* (2020)
O. unilateralis s. l.	OSC 128574	DQ522554	DQ522339	DQ522385	DQ522436	Unidentified ant	Thailand	Spatafora *et al.* (2007)
	P.M1	—	MN218244	—	—	*Polyrhachis moesta*	Taiwan	Lin *et al.* (2020)
	P.M2	—	MN218245	—	—	*Polyrhachis moesta*	Taiwan	Lin *et al.* (2020)
	P.M3	—	MN218246	—	—	*Polyrhachis moesta*	Taiwan	Lin *et al.* (2020)
	P.W1	—	MN218247	—	—	*Polyrhachis wolfi*	Taiwan	Lin *et al.* (2020)
	P.W2	—	MN218248	—	—	*Polyrhachis wolfi*	Taiwan	Lin *et al.* (2020)
	P.W3	—	MN218249	—	—	*Polyrhachis wolfi*	Taiwan	Lin *et al.* (2020)
	P.V1	—	MN218253	—	—	*Polyrhachis vigilans*	Taiwan	Lin *et al.* (2020)
	P.V2	—	MN218254	—	—	*Polyrhachis vigilans*	Taiwan	Lin *et al.* (2020)
	P.V3	—	MN218255	—	—	*Polyrhachis vigilans*	Taiwan	Lin *et al.* (2020)
	P.L1	—	MN218250	—	—	*Polyrhachis latona*	Taiwan	Lin *et al.* (2020)
	P.L2	—	MN218251	—	—	*Polyrhachis latona*	Taiwan	Lin *et al.* (2020)
	P.L3	—	MN218252	—	—	*Polyrhachis latona*	Taiwan	Lin *et al.* (2020)
	P.De1	—	MN218259	—	—	*Polyrhachis debilis*	Taiwan	Lin *et al.* (2020)
	P.De2	—	MN218260	—	—	*Polyrhachis debilis*	Taiwan	Lin *et al.* (2020)
	P.De3	—	MN218261	—	—	*Polyrhachis debilis*	Taiwan	Lin *et al.* (2020)
	P.I1	—	MN218256	—	—	*Polyrhachis illaudata*	Taiwan	Lin *et al.* (2020)
	P.I2	—	MN218257	—	—	*Polyrhachis illaudata*	Taiwan	Lin *et al.* (2020)
	P.I3	—	MN218258	—	—	*Polyrhachis illaudata*	Taiwan	Lin *et al.* (2020)
	P.Di1	—	MN218262	—	—	*Polyrhachis dives*	Taiwan	Lin *et al.* (2020)
	P.Di2	—	MN218263	—	—	*Polyrhachis dives*	Taiwan	Lin *et al.* (2020)
	P.Di3	—	MN218264	—	—	*Polyrhachis dives*	Taiwan	Lin *et al.* (2020)
	C.P1	—	MN218240	—	—	*Camponotus punctatissimus*	Taiwan	Lin *et al.* (2020)
	C.P2	—	MN218241	—	—	*Camponotus punctatissimus*	Taiwan	Lin *et al.* (2020)
	C.P3	—	MN218242	—	—	*Camponotus punctatissimus*	Taiwan	Lin *et al.* (2020)
	C.P4	—	MN218243	—	—	*Camponotus punctatissimus*	Taiwan	Lin *et al.* (2020)
	Gh41	KX713656	KX713668	KX713706	—	*Polyrhachis* sp.	Ghana	Araújo *et al.* (2018)

Table 1. (Continued).

Current species	Voucher	18S	*TEF1*	*RPB1*	*RPB2*	Host species	Country	Reference
	MF154	MK874745	MK863823	—	—	*Camponotus* sp.	—	Araújo *et al.* (2020)
O. unilateralis s. str.	SERI1	KX713628	KX713675	KX713730	—	*Camponotus sericeiventris*	Brazil	Evans *et al.* (2018)
	SERI2	KX713627	KX713676	KX713731	—	*Camponotus sericeiventris*	Brazil	Evans *et al.* (2018)
Ophiocordyceps (Hirsutella) sp.	NHJ 12525	EF469125	EF469063	EF469092	EF469111	*Hemiptera*	—	Sung *et al.* (2007)
	OSC 128575	EF469126	EF469064	EF469093	EF469110	*Hemiptera*	—	Sung *et al.* (2007)

Table 2. Comparison of hosts, morphological characters, and geographic distribution of the myrmecophilous species of the *Ophiocordyceps unilateralis* complex, *O. kniphofioides* complex, and related species. New species described in this work in **bold**. *Asexual morph with macro and microconidia, ***Paraisaria* type asexual morph, *** Stilbelliformis type sexual morph.

***Ophiocordyceps* spp.**	**Hosts**	**Death position**	**Ascospores**			**Hirsutella type**			**Complex**	**Distribution**	**Reference(s)**
			Size (µm)	**Capilliconidiophore (longitude µm)**	**Septa**	**A**	**B**	**C**			
O. acroasca	*Camponotus* sp.	Biting leaves	83–108 × 2–3	—	4–5	x	—	x	*O. unilateralis*	China	Tang *et al.* (2023b)
O. albacongiuae	*Camponotus* sp.	Biting epiphytes and base of trees	80–100 × 5	—	5–6	—	—	—	*O. unilateralis*	Colombia	Araújo *et al.* (2018)
O. ansiformis	*Colobopsis* sp.	Biting leaves	45–59 × 5–6	60–79	6–9	x	—	—	*O. unilateralis*	China	Tang *et al.* (2023c)
O. basiasca	*Camponotus* sp.	Biting leaves	89–119 × 2–3	—	4–5	x	—	—	*O. unilateralis*	China	Tang *et al.* (2023b)
O. blakebarnesii	*Camponotus* cf. *chromaiodes*	Biting into logs	140–160 × 4	—	6–7	x	—	—	*O. unilateralis*	EUA	Araújo *et al.* (2018)
O. bifertilis	*Polyrhachis* spp.	Biting leaves	70–94 × 2–4	—	4–5	x	—	—	*O. unilateralis*	China	Tang *et al.* (2023b)
O. camponoti-atricipis	*Camponotus atriceps*	Biting leaves	80–85 × 3	55	5	x	—	—	*O. unilateralis*	Brazil	Araújo *et al.* (2015)
O. camponoti-balzani	*Camponotus balzani*	Biting leaves	135–174 × 4–5	—	14–22	x	—	x	*O. unilateralis*	Brazil	Evans *et al.* (2011a, b)
O. camponoti-bispinosi	*Camponotus bispinosus*	Biting the tip of palm leaf	70–75 × 4.5	65	4–5	x	—	—	*O. unilateralis*	Brazil	Araújo *et al.* (2015)
O. camponoti-chartificis	*Camponotus chartifex*	Biting the tip of palm leaf	75–85 × 5	75–90	9–13	x	—	—	*O. unilateralis*	Brazil	Araújo *et al.* (2018)
O. camponoti-femorati	*Camponotus femoratus*	Biting the tip of palm leaf	75–90 × 3	35–40	5	x	—	—	*O. unilateralis*	Brazil	Araújo *et al.* (2018)
O. camponoti-floridani	*Camponotus floridanus*	Biting the tip of palm leaf	75–90 × 4–5	—	5	x	—	—	*O. unilateralis*	EUA	Araújo *et al.* (2018)

Table 2. (Continued).

Ophiocordyceps spp.	Hosts	Death position	Ascospores			Hirsutella type			Complex	Distribution	Reference(s)
			Size (µm)	Capilliconidiophore (longitude µm)	Septa	A	B	C			
O. camponoti-hippocrepidis	*Camponotus hippocrepis*	Biting spines	75–85 × 4–5	45–50	5	x	—	—	*O. unilateralis*	Brazil	Araújo *et al.* (2018)
O. camponoti-indiani	*Camponotus indianus*	Biting leaves	75 × 4.5	130	5	x	—	x	*O. unilateralis*	Brazil	Araújo *et al.*(2015)
O. camponoti-leonardi	*Colobopsis leonardi*	Biting leaves	110–125 × 2–3	—	7–8	x	—	x	*O. unilateralis*	Thailand	Kobmoo *et al.* (2012, 2015)
O. camponoti-melanotici	*Camponotus melanoticus*	Biting leaves	170–210 × 4–5	—	27–35	x	—	—	*O. unilateralis*	Brazil	Evans *et al.* (2011a, b)
O. camponoti-nidulantis	*Camponotus nidulans*	Biting sapling leaves and petioles	90–105 × 3–4	50–60	5	x	—	x	*O. unilateralis*	Brazil	Araújo *et al.* (2018)
O. camponoti-novogranadensis	*Camponotus novogranadensis*	Biting epiphytic lichens	75–95 × 2.5–3.5	20–25	5–10	x	x	—	*O. unilateralis*	Brazil	Evans *et al.*(2011a)
O. camponoti-renggeri	*Camponotus renggeri*	Biting leaves and moss	90–120 × 4	—	5–8	—	—	x	*O. unilateralis*	Brazil	Araújo *et al.* (2018)
O. camponoti-rufipedis	*Camponotus rufipes*	Biting leaves	80–95 × 2–3	60–70	4–7	x	—	—	*O. unilateralis*	Brazil	Evans *et al.* (2011a, b)
O. camponoti-saundersi	*Camponotus saundersi*	Biting leaves	75–85 × 2–3	—	7–8	x	—	x	*O. unilateralis*	Thailand	Kobmoo *et al.* (2012, 2015)
O. camponoti-sexguttati	*Camponotus sexguttatus*	Biting the tip of palm leaf	120–140 × 3	25–30	7	x	—	—	*O. unilateralis*	Brazil	Araújo *et al.* (2018)
O. camponoti-striati	***Camponotus striatus* s. l.**	**Biting twigs, shrubs and vines**	**102–148 × 2.8–3.5**	**—**	**12–21**	**x**	**—**	**x**	***O. unilateralis***	**Mexico**	**This study**
O. cephalotiphila	***Cephalotes goniodontus* & *Cephalotes hirsutus***	**Biting the base and roots of trees**	**79.5–109 × 2.5–3**	**37–79**	**5**	**x**	**—**	**x**	***O. unilateralis***	**Mexico**	**This study**
O. contiispora	*Camponotus* sp.	Biting leaves	38–48 × 2–4	—	No obvious separation	—	—	x	*O. unilateralis*	China	Tang *et al.* (2023b)
O. deltoroi	***Camponotus sericeiventris* s. l. & *C. tepicanus***	**Biting the base of trees, roots, rocks**	**82–131 × 2–3**	**—**	**5**	**x**	**—**	**x**	***O. unilateralis***	**Mexico**	**This study**
O. desmidiospora	*Camponotus brutus*, *C. pennsylvanicus* (queens)	Into logs, abnormal behavior	—	—	—	*			—	Ghana, EUA	Evans & Samson (1984); Saltamachia & Araújo (2020)
O. flabellata	*Camponotus* sp.	Biting leaves	76–116 × 2–3	—	3–4	x	—	—	*O. unilateralis*	China, Vietnam	Tang *et al.* (2023a)
O. fusiformispora	*Polyrhachis* sp.	Biting leaves	—	—	—	x	—	—	*O. unilateralis*	China	Lu *et al.* (2024)

Table 2. (Continued).

Ophiocordyceps spp.	Hosts	Death position	Ascospores			Hirsutella type			Complex	Distribution	Reference(s)
			Size (µm)	Capilliconidiophore (longitude µm)	Septa	A	B	C			
O. halabalaensis	*Dinomyrmex gigas*	Biting leaves	60–75 × 3–5	—	7–8	x	—	—	*O. unilateralis*	Thailand	Luangsa-ard *et al.* (2011)
O. haraveriensis	***Camponotus atriceps* s. l.**	**Biting trunks, branches, roots, rocks**	**81.6–146 × 2–2.5**	**21.5–36.5**	**7**	**x**	**—**	**x**	***O. unilateralis***	**Mexico**	**This study**
O. jaliscana	***Colobopsis* sp. & *Camponotus tepicanus***	**Biting trunks, branches, green twigs, roots**	**63−112 × 2−2.5**	**52–67.5**	**5**	**x**	**—**	**x**	***O. unilateralis***	**Mexico**	**This study**
O. kimflemingiae	*Camponotus castaneus* & *C. americanus*	Biting twigs	80–90 × 5	80–100	5–6	x	—	x	*O. unilateralis*	EUA	Araújo *et al.* (2018); Loreto *et al.* (2018); Saltamachia & Araújo (2020)
O. lilacina	*Polyrhachis* sp.	Biting leaves	—	—	—	x	—	—	*O. unilateralis*	China	Tang *et al.* (2023a)
O. naomipierceae	*Polyrhachis* cf. *robsonii*	Biting leaves	75–105 × 5–6	—	4–6	**			*O. unilateralis*	Australia	Araújo *et al.* (2018)
O. nooreniae	*Polyrhachis lydiae* and *Polyrhachis* cf. *hookeri*	Biting leaves	—	—	—	x	—	x	*O. unilateralis*	Australia	Crous *et al.* (2016)
O. nuozhaduensis	*Camponotus* sp.	Biting leaves	91–126 × 2–5	—	7–13	x	—	—	*O. unilateralis*	China	Tang *et al.* (2023b)
O. oecophyllae	*Oecophylla smaragdina*	Biting leaves	—	—	—	—	—	x	—	Australia	Araújo *et al.* (2018)
O. ootakii	*Polyrhachis moesta*	Biting leaves	85–100 × 3	—	5	x	—	—	*O. unilateralis*	Japan	Araújo *et al.* (2018)
O. polyrhachis-furcata	*Polyrhachis furcata*	Biting leaves	90–100 × 2–3	—	—	x	—	x	*O. unilateralis*	Thailand	Kobmoo *et al.* (2012, 2015)
O. pseudocamponoti-atricipis	***Camponotus atriceps* s. l.**	**Biting leaves**	**80–108 × 2–2.5**	**30–58**	**5**	**x**	**—**	**—**	***O. unilateralis***	**Mexico**	**This study**
O. pulvinata	*Camponotus obscuripes*	Biting twigs	160-220 × 3-5; 123–248 × 2.8–4.7	—	10–15	—	—	—	*O. unilateralis*	Japan	Kepler *et al.* (2011); Kaitsu *et al.* (2013)
O. rami	*Camponotus* sp.	Biting green twigs	200–215 × 2–3	—	7–8	x	—	x	*O. unilateralis*	Thailand	Kobmoo *et al.* (2015)
O. satoi	*Polyrhachis lamellidens*, and others *Polyrhachis* spp.	Biting twigs	85–100 × 4; 90–114 × 2–3	40–50; 89–104	3–5	x	—	x	*O. unilateralis*	Japan, China	Araújo *et al.* (2018); Tang *et al.* (2023a)
O. septa	*Camponotus* sp.	Biting leaves	45–50 × 6–8	—	7–8	x	—	x	*O. unilateralis*	Thailand	Kobmoo *et al.* (2015)

Table 2. (Continued).

Ophiocordyceps spp.	Hosts	Death position	Ascospores			Hirsutella type			Complex	Distribution	Reference(s)
			Size (µm)	Capilliconidiophore (longitude µm)	Septa	A	B	C			
O. (*Hirsutella*) *sporodochialis*	*Polyrhachis militaris*, *P laboriosa*, *P. decemdentata*, *P. revoili*	Biting twigs	—	—	—	—	—	x	*O. unilateralis*	Ghana	Evans & Samson (1984)
O. subtiliphialida	*Camponotus* sp.	Biting leaves	52–72 × 5–7	58–79	6–7	—	—	x	*O. unilateralis*	China	Tang *et al.* (2023b)
O. tianshanensis	*Camponotus japonicus*	Without a biting behavior on decayed wood	—	—	—	x	—	—	*O. unilateralis*	China	Wei *et al.* (2020)
O. tortuosa	*Colobopsis* sp.	Biting leaves	47–64 × 5–7	44–65	6–7	x	—	x	*O. unilateralis*	China	Tang *et al.* (2023c)
O. unilateralis s.str.	*Camponotus sericeiventris sericeiventris*	Biting leaves	75–85 x 2-2.5	—	4–5	x	—	x	*O. unilateralis*	Brazil, Colombia	Evans *et al.* (2018); Loreto *et al.* (2018)
Ophiocordyceps sp.	*Camponotus sericeiventris*	Biting the base of trees	—	—	—	x	—	x	*O. unilateralis*	Honduras	Evans & Samson (1984)
Ophiocordyceps sp.	*Polyrhachis militaris*	Biting trunks	—	—	—	—	—	—	*O. unilateralis*	Ghana	Araújo *et al.* (2018)
Ophiocordyceps sp.	*Polyrhachys mesota*, *P. wolfi*, *P. vigilans*, *P. latona*, *P. debilis*, *P. illaudata*, *P. dives* & *Camponotus punctatissimus*	Biting leaves	—	—	—	—	—	—	*O. unilateralis*	Taiwan	Lin *et al.* (2020)
Ophiocordyceps sp.	*Camponotus pennsylvanicus*	Biting the base of trees, between moss	—	—	—	—	—	—	*O. unilateralis*	EUA	Saltamachia & Araújo (2020)
O. daceti	*Daceton armigerum*	Without a biting behavior on leaves	—	—	—	x	—	—	*O. kniphofioides*	Brazil	Araújo *et al.* (2018)
O. dolichoderi	*Dolichoderus attelaboides*	Between fallen leaves	—	—	—	x	***		*O. kniphofioides*	Brazil	Evans & Samson (1982); Araújo *et al.* (2018)
O. kniphofioides	*Cephalotes atratus*	Base of trees	110–150 × 1.5–3	—	3–5	x	***		*O. kniphofioides*	Brazil, Colombia	Evans & Samson (1982); Sanjuan *et al.* (2015); Araújo *et al.* (2018)
O. monacidis	*Dolichoderus bispinosus*	Base of trees (with moss)	95–110 × n/d	—	3–4	x	—	—	*O. kniphofioides*	Brazil	Evans & Samson (1982); Araújo *et al.* (2018)
O. ponerinarum	*Paraponera clavata*	Base of trees	—	—	—	x	—	—	*O. kniphofioides*	Brazil, Colombia	Evans & Samson (1982); Sanjuan *et al.* (2015)

bark or non-woody stems, 27 Sep. 2019, *C.E. Ballesteros-Aguirre* 993 (SC232) (**holotype** IBUG–15426; GenBank 18S: PV745528, *TEF1*: PV759174, *RPB1*: PV759211) (see Tables S1 & S2 for additional information). **Paratypes**, idem., *C.E. Ballesteros-Aguirre* 145, 146, 215 (SC123), 1132, 1282 (SC231), 1752 (SC235) (IBUG) (see Table S1 for specimen information).

External mycelium scant to abundant, white to pale brown with age; emerges from the ant's intersegmental membranes, adhering ventrally to the substrate. *Stroma* solitary, cylindrical to thread-like, usually unbranched, tomentose to velutinous at the base, velutinous after the perithecial cushion towards the apex, black to pale brown towards the base, 7.5–20 mm long, 150–230 µm wide at base, 100–118 µm wide at apex, grows dorsally between the head and dorsal pronotum. *Perithecial cushions* 1–2, hemispherical, rough at maturity due to the perithecial ostioles, black, 0.64–0.74 × 0.50–0.69 mm, formed unilaterally on the stroma. *Perithecia* sub-immersed, lageniform, neck short, 300–352 × 85–184 µm, perpendicular to the surface of the stroma. *Asci* cylindrical to clavate, base thinned, hyaline, 125–188 × 8–12 µm, apical region 4.5–6.5 × 5–6 µm, with 8 ascospores. *Ascospores* filiform, straight to slightly curved, with one end slightly rounded and the other tapering towards the end, with 12–21 septa, thin-walled, hyaline, (94–)102–148 × 2.8–3.5(–4) µm.

Ascospore germination: It was attempted, but germination was not achieved.

Asexual morphs: *Hirsutella type A* on the apical part of the stroma. *Phialides* lageniform, hyaline, base 4–7(–10) × 2.4–4.5 µm, with flexuous neck, 3.5–7(–16.8) × 0.5–0.8 µm, emerge directly from the stromal hyphae. *Conidia* narrow to broad spindle-shaped, some apiculated, hyaline, 4–6.8 × 1.5–2.5 µm, emerge from the neck of phialides. *Hirsutella type C* forming brown *sporodochia*, emerging from intersegmental membranes of antennae, legs, and other body parts of ants, or directly on the external mycelium attached to the substrate. *Phialides* narrowly lageniform, some sub-cylindrical, gradually tapering into a long neck, cylindrical, flexuous, hyaline, base (4.5–)6–21 × 2.5–6 µm, neck 15.5–28.5 × 1.2–2 µm. *Conidia* cylindrical to narrowly spindle-shaped, without apicule, ends rounded to acute, hyaline, without mucus, 13–17 × 2.5–3 µm, formed at the tip of the phialides.

Distribution: Only known from west of Jalisco state, Mexico.

Habitat and ecology: Tropical forests, small epizootics in GF and TMCF. Host is an undescribed species of the *Camponotus striatus* complex, here named *Camponotus* sp. 1. Ants die biting the bark of twigs or on non-woody stems, scattered on shrubs and vines. Zombie-ant fungi closest to the forest floor at a height of 45–100 cm and the farthest at a height of 1.6–1.76 m (n = 2 ant graveyards).

Ophiocordyceps cephalotiphila C.E. Ballesteros-Aguirre, T. Sanjuan & L. Guzmán-Dávalos, ***sp. nov.*** MB 859566. Fig. 5.

Etymology: The specific epithet refers to the fact that this species of *Ophiocordyceps* has affinity by *Cephalotes*.

Typus: **Mexico**, west of Jalisco state, road to Haravéri Botanical Garden, 20°45'48.3"N, 104°57'14.6"W, 857 m.a.s.l., subdeciduous tropical forest, host *Cephalotes hirsutus* (*Myrmicinae*: *Attini*), minor and major workers, ants die biting the bark on the base of trees or shrubs, sometimes stems or branches, 24 Oct. 2020, *C.E. Ballesteros-Aguirre* 1216 (SC156) (**holotype** IBUG–15427; GenBank 18S: PV745532, *TEF1*: PV759176, *RPB1*: PV759215, *RPB2*: PV759197) (see Tables S1 & S2 for additional information). **Paratypes**, idem., *C.E. Ballesteros-Aguirre* 1025, 1155, 1213 (SC155 & SC334), 1218 (SC157), 1219, 1223, 1257 (SC182), 1258 (SC183), 1260, 1261 (SC191), 1303 (SC333), 1305, 1322, 1323, 1324, 1325, 1326, 1327 (IBUG) (see Table S1 for specimen information).

External mycelium scant, pale brown to reddish brown; emerges between intersegmental membranes of legs and mesosoma of the host, but more abundant on mandibles and ventral area of gaster, adhering to the substrate. *Stroma* solitary, cylindrical, with broadened base, gradually acute towards the apex, frequently branched, tomentose to velutinous at the base, velutinous towards the apex, pale brown to black at the base, grey to purple towards the apex, 6–14 mm long, 190–550 µm wide at base, 50–75(–140) µm wide at apex, grows dorsally between the pronotum and head. *Perithecial cushions* 1–4 (or more), hemispherical, rough at maturity due to prominent perithecial ostioles, brown to black, 0.5–1 × 0.5–1.2 mm, unilateral on the stroma. *Perithecia* sub-immersed, lageniform, 183–408 × (82–)160–200 µm, neck long, perpendicular to the surface of the stroma. *Asci* cylindrical to clavate, base thinned, hyaline, (120–)144–194 × (6–)7.3–10.5 µm, apical region 3–7.5 × 4.5–5.5 µm, with 8 ascospores. *Ascospores* filiform, curved to sigmoidal, rarely straight, ends sharp, with 5(–7) septa, thin-walled, hyaline, 79.5–109(–113.5) × (2–)2.5–3(–3.5) µm.

Ascospore germination: 1–3 capilliconidiophores, thread-like, straight, (22.5–)37–79 × 1–1.5 µm; each capilliconidiophore bearing a single capilliconidium, ovoid to allantoid, narrowing apically, smooth-walled, hyaline, covered with mucus, 6–10 × 2–4 µm.

Asexual morphs: *Hirsutella* types A and C on the same hymenium, in main stroma and in synnemata. *Synnemata* cylindrical, simple or branched, emerge from the external mycelium of the gaster and on the body of the ants. *Hirsutella type A* on the apical part of the stroma, after the perithecial cushion or towards the apex on synnemata. *Phialides* lageniform, hyaline, base (3.5–)4.5–11 × 2.5–4.5 µm, neck flexuous, 6–12.5 × 0.5–1 µm. *Conidia* fusiform, with or without apiculus, hyaline, 4.5–8.5(–10) × 1.5–3.2 µm, emerge from the neck of the phialides. *Hirsutella* type C at the base of the stroma, gradually disappearing as the presence of *Hirsutella* type A phialides increases towards the apex; also forming brown sporodochia that emerge from intersegmental membranes of antennae, legs, and sometimes on other body parts of the ants or on the surface of the perithecial cushions. *Conidiophores* of variable complexity. *Phialides* narrowly lageniform, some sub-cylindrical, gradually tapering into a long neck, cylindrical, flexuous, hyaline, base 7.5–17(–19.5) × 2–4(–5.5) µm, neck 12–32(–38) × 0.5–1(–2) µm. *Conidia* cylindrical to narrowly spindle-shaped, without apicule, ends

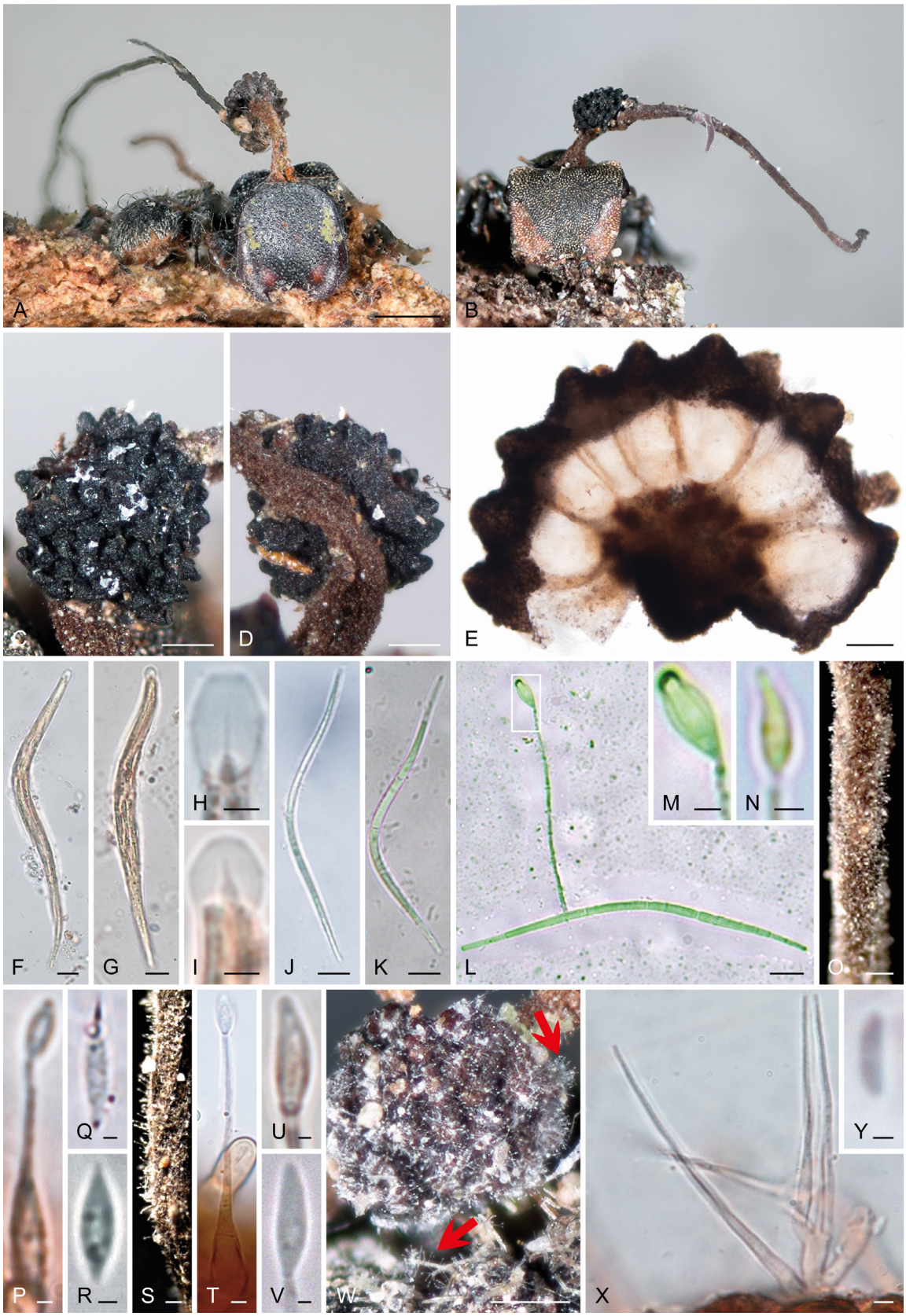

Fig. 5. *Ophiocordyceps cephalotiphila* (A, E, F, H, J, O–Q, S–U, W–Y: C.E. Ballesteros-Aguirre 1216 (SC156), holotype; B–D, R, V: C.E. Ballesteros-Aguirre 1213 (SC155 & SC334); G, I: C.E. Ballesteros-Aguirre 1155; K: C.E. Ballesteros-Aguirre 1327; L–M: C.E. Ballesteros-Aguirre 1326; N: C.E. Ballesteros-Aguirre 1325). **A, B.** Hosts *Cephalotes hirsutus* and *Ceph. goniodontus* (both major workers), biting the bark at the base of a tree with a stroma emerging between the pronotum and head, with a perithecial cushion. **C, D.** Unilaterally attached perithecial cushion produced from the stroma. **E.** Cross-section of perithecial cushion showing the perithecial arrangement. **F, G.** Asci. **H, I.** Apical region of the asci. **J, K.** Ascospores with five septa one week after being released on a slide in a humid chamber. **L.** Ascospore germinating in a capilliconidiophore, one week after being released on a slide in a humid chamber. **M, N.** Close-up of the capilliconidium, **M.** with mucus around it, **N** without mucus after being stained. **O–R.** Asexual morph *Hirsutella* type A. **O.** Phialides and conidia from the stromal apex. **P.** Phialide with conidium. **Q, R.** Conidia. **S–Y.** Asexual morph *Hirsutella* type C. **S.** Phialides from the stromal base. **T.** Phialide from the stromal base, with conidium. **U, V, Y.** Conidia. **W.** Unilateral perithecial cushion and ant's body with phialides and conidia (red arrows). **X.** Phialides from the perithecial cushion. Scale bars: A, B = 1 mm; C, D, W = 250 µm; E = 100 µm; O, S = 50 µm; F, G, J–L = 10 µm; H, I, M, N, T, X = 2.5 µm; P–R, U, V, Y = 1 µm.

rounded, hyaline, with mucus before staining, 3–9.5 × 1.2–3(–4.3) µm, emerge from the neck of the phialides.

Distribution: Only known from west of Jalisco state, Mexico.

Habitat and ecology: Tropical forests, epizootics mainly in SDTF, but also present in GF. The fungus was found infecting two species of *Cephalotes*, *Ceph. goniodontus* and *Ceph. hirsutus*. Ants die biting the bark mainly at the bases, or sometimes higher up, of trees and shrubs, or biting exposed roots. It is common to find individuals very close together in the ant graveyards. Zombie-ant fungi closest to the forest floor at a height of (0.5–)2–10(–15) cm and the farthest at a height of 0.3(–3.1) m (n = 10 ant graveyards).

Ophiocordyceps deltoroi C.E. Ballesteros-Aguirre, T. Sanjuan & L. Guzmán-Dávalos, ***sp. nov.*** MB 859581. Fig. 6.

Etymology: The specific epithet is in honour of Guillermo Del Toro, a Mexican filmmaker born in the Jalisco state, famous for his fantastic movie characters.

Typus: **Mexico**, west of Jalisco state, nearby Haravéri Botanical Garden, 20°45'33.9"N, 104°57'46"W, 810 m.a.s.l., tropical montane cloud forest, host *Camponotus sericeiventris* s. l. (*Camponotus* sp. 2) (*Formicinae*: *Camponotini*), minor and major workers, ants die biting the base of trees or shrubs, exposed roots, on the bark or the inferior surface of the rocks, 24 Oct. 2020, *C.E. Ballesteros-Aguirre* 1227 (SC162) (**holotype** IBUG–15428; GenBank 18S: PV745537, *TEF1*: PV759182, *RPB1*: PV759220) (see Tables S1 & S2 for additional information). **Paratypes**, idem., *C.E. Ballesteros-Aguirre* 602, 1147, 1211 (SC236), 1224 (SC159), 1225 (SC160), 1226 (SC161), 1251 (SC177), 1263 (SC192) (IBUG) (see Table S1 for specimen information).

External mycelium scant to abundant, sometimes covering the host, initially white, gradually turning pale brown or reddish; emerges from the ant's intersegmental membranes, concentrated on the ventral host area and mandibles, adhering to the substrate. *Stromata* 1–3, thread-like, with broadened base, gradually acute towards the apex, simple or branched, tomentose to hirsute at the base and towards the perithecial cushion, velutinous towards the apex, black to reddish brown at the base, purple towards the apex, 5–26.7 mm in length, 300-648 (-800) µm width at base, 68–110 µm width at apex, grows dorsally between head and pronotum, or laterally on the sides of the mesonotum. *Perithecial cushions* 1–3(–5), hemispherical to ovoid, rough at maturity due to prominent perithecial ostioles, black, sometimes dark brown, 0.94–2 × 0.9–1.5 mm, larger in major workers and soldiers, unilaterally attached on variable places on the stromata; sometimes two perithecial cushions emerge at the same level, giving the appearance of completely surrounding the stroma. *Perithecia* sub-immersed, lageniform, neck short, (347–)376–456 × 113–224 µm, perpendicular to the surface of the stroma. *Asci* cylindrical to clavate, base thinned, hyaline, 150–190 × 7–10 µm, apical region 3.5–6.4(–8) × 4–7.5 µm, with 8 ascospores. *Ascospores* filiform, curved to sigmoidal, rarely straight, ends sharp, with 5 septa, thin-walled, hyaline, (68–)82–131 × 2–3 µm.

Ascospore germination: It was attempted, but germination was not achieved.

Asexual morphs: *Hirsutella* types A and C on the same hymenium, in main stromata and synnemata. *Synnemata* cylindrical, simple to branched, 3.5–15 mm in length, 40–195 µm width at base, 40–70 µm width at apex, grow on the tarsi and intersegmental membranes of legs and antennae. In *Camponotus* sp. 3 only with a main synnema that emerge dorsally between head and pronotum, without perithecial cushion (Fig. 6C). *Hirsutella type A* on the apical part of the stroma, after the perithecial cushion or towards the apex on synnemata. *Phialides* lageniform or cylindrical, straight, brown, base (3.2–)7–13.6 × 2.5–4.8 µm, neck 4.8–11.2(–13.6) × 0.4–1 µm, or neckless. *Conidiogenous* hyphae cylindrical, septate, hyaline, in the hymenium. *Conidia* fusiform, some apiculate, hyaline or brown, 5–7.5 × 2–3 µm, emerge from the neck of phialides or in clusters from the apical part of neckless phialides and from conidiogenous hyphae. *Hirsutella* type C at the base of the stroma, gradually disappearing as the presence of *Hirsutella* type A phialides increases towards the apex; also forming brown sporodochia (Fig. 6O) that emerge from intersegmental membranes of antennae, legs, and other body parts of ants. *Conidiophores* of variable complexity. *Phialides* narrowly lageniform, some cylindrical to thread-like (Figs 2G, 6O–R), hyaline, base (8–)14–26.5(–30) × 3.2–5(–7.5) µm, gradually tapering into a long, cylindrical, neck flexuous, (17.3–)30–78 × 1.2–2 µm. *Conidia* cylindrical to narrowly spindle-shaped, without apicule, ends rounded, hyaline, with mucus that is lost when rehydrated, 7.5–13.5(–15.2) × (2–)2.5–3.2 µm, emerge from the neck of the phialides.

Distribution: Only known from west of Jalisco state, Mexico.

Habitat and ecology: Tropical forests, large epizootics in the TMCF. Hosts undescribed species of the *Camponotus sericeiventris* and *Camp. tepicanus* complexes, here named *Camponotus* sp. 2 and *Camponotus* sp. 3, respectively. Ants die biting the bark at the base of trees or shrubs, exposed roots, and the base of the rocks. Most of the specimens of zombie-ant fungi on *Camponotus* sp. 2 with immature perithecial cushions, with a large number of synnemata and numerous sporodochia in various parts of the ant's body, with few mature specimens compared to the number of samples collected. Zombie-ant fungi in *Camponotus* sp. 3 only with asexual stromata. Sometimes fungi and hosts covered in sediment, with only the stroma visible. Zombie-ant fungi closest to the forest floor at a height of 2–11 cm and the farthest at a height of 0.86–0.96(–2.56) m (n = 7 ant graveyards, 5 of Camponotus sp. 2 and 2 of Camponotus sp. 3).

Ophiocordyceps haraveriensis C.E. Ballesteros-Aguirre, L. Guzmán-Dávalos & T. Sanjuan, ***sp. nov.*** MB 859582. Fig. 7.

Etymology: The specific epithet refers to the type locality, the Haravéri Botanical Garden.

Typus: **Mexico**, west of Jalisco state, nearby Haravéri Botanical Garden, Hacienda Las Tres Carmelitas,

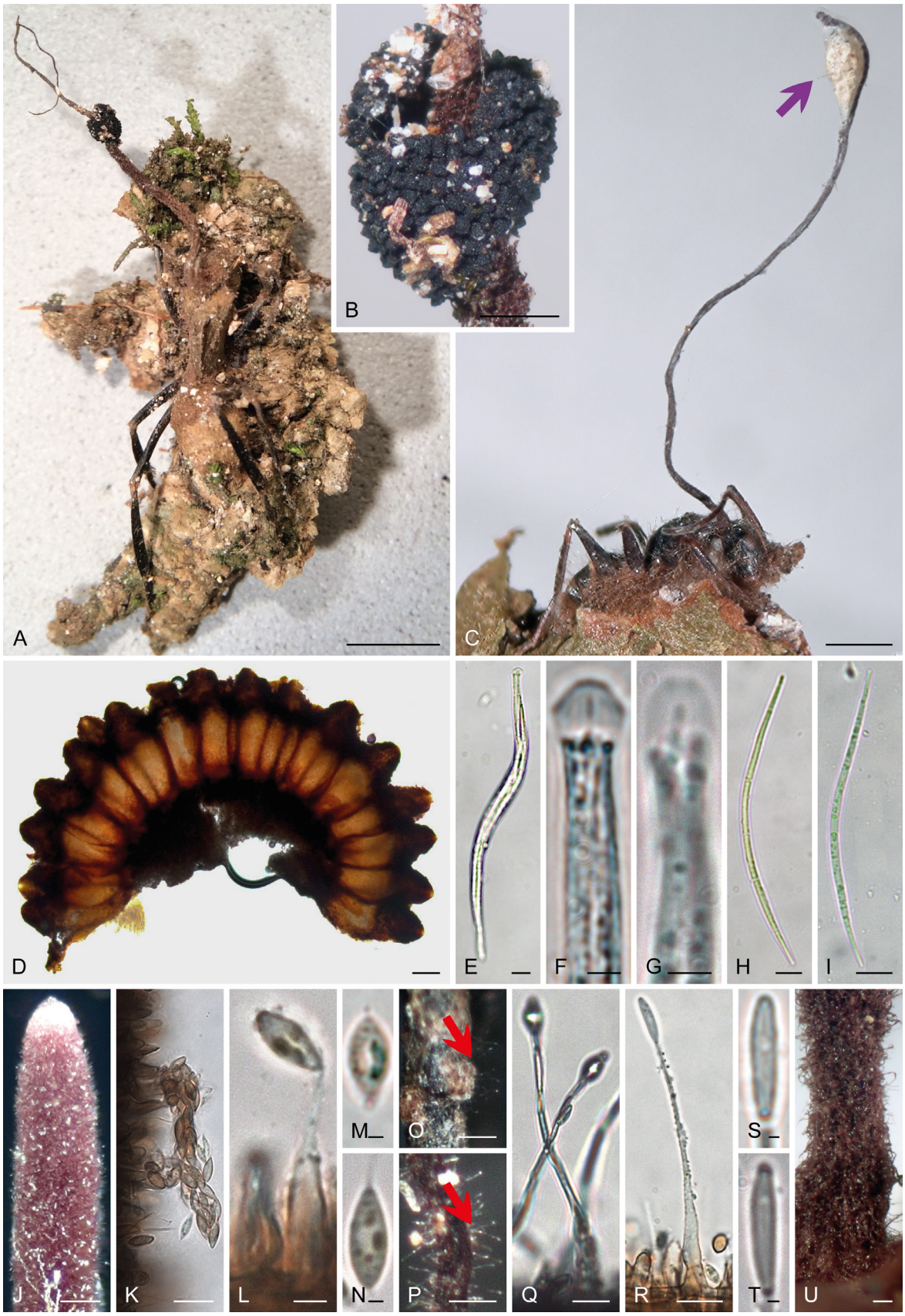

Fig. 6. *Ophiocordyceps deltoroi* (A, B, D–F, H, J, M, S, U: C.E. Ballesteros-Aguirre 1227 (SC162), holotype; C: C.E. Ballesteros-Aguirre 1263 (SC192); G, I, O: C.E. Ballesteros-Aguirre 602; K, L, N, P–R, T: C.E. Ballesteros-Aguirre 1147). **A.** Host *Camponotus* sp. 2 (*Camp. sericeiventris* s. l.) biting the bark at the base of a tree with a stroma emerging between the pronotum and head, with perithecial cushion. **B.** Two unilateral perithecial cushions produced at the same level from the stroma. **C.** Host *Camponotus* sp. 3 (*Camp. tepicanus* s. l.) biting the bark at the base of a tree with an asexual stroma emerging between the pronotum and head; with a pupa of an undetermined insect (purple arrow) commonly associated. **D.** Cross-section of the perithecial cushion showing the perithecial arrangement. **E.** Ascus. **F, G.** Apical region of the asci. **H, I.** Ascospores, in **H.** with five septa visible. **J–N.** Asexual morph *Hirsutella* type A. **J.** Apex of the stroma. **K.** Phialides from the stromal apex with a conidial mass. **L.** Phialide with conidium. **M, N.** Conidia. **O–T.** Asexual morph *Hirsutella* type C. **O.** Sporodochia on an ants' antenna. **P.** Phialides from the stromal base. **Q.** Phialides with mucus before stain. **R.** Phialide with a conidium. **S, T.** Conidia. **U.** Stromal base with age. Scale bars: A = 5 mm; B = 0.5 mm; C = 1 mm; D, O–P = 100 µm; J = 50 µm; E, H–I, K, Q–R = 10 µm; L = 2.5 µm; M–N, S–T = 1 µm.

Fig. 7. *Ophiocordyceps haraveriensis* (A–G, I, M–V: C.E. Ballesteros-Aguirre 1247 (SC173), holotype; H: C.E. Ballesteros-Aguirre 127 (SC127); J: C.E. Ballesteros-Aguirre 1317; K–L: C.E. Ballesteros-Aguirre 1316; W: C.E. Ballesteros-Aguirre 129). **A.** Host *Camponotus* sp. 4 (*Camp. atriceps* s. l.) biting the bark of a trunk with a stroma emerging between the pronotum and head, with three perithecial cushions. **B–D.** Unilateral perithecial cushion produced from the stroma, in **B.** with two unilateral perithecial cushions produced at the same level. **E.** Cross-section of the perithecial cushion showing the perithecial arrangement. **F.** Asci. **G, H.** Apical region of the asci, **I, J.** Ascospores with seven septa, **J.** released on a slide in a humid chamber. **K.** Ascospore germinating one week after being released in a capilliconidiophore and exhibiting a swollen region. **L.** Close-up of capilliconidium. **M–Q.** Asexual morph *Hirsutella* type A. **M.** Apex of a developing stroma. **N.** Apex of a fixed stroma. **O.** Phialide. **P, Q.** Conidia. **R–V.** Asexual morph *Hirsutella* type C. **R.** Base of a developing stroma. **S, T.** Phialides. **U, V.** Conidia. **W.** Stromal base with age. Scale bars: A = 1 mm; B, D = 250 µm; E, M, R, W = 100 µm; N = 25 µm; F, I–K, S, T = 10 µm; L = 5 µm; G, H, O = 2.5 µm; P, Q, U, V = 1 µm.

20°45’33.2”N, 104°58’5.6”W, 762 m.a.s.l., gallery forest, host *Camponotus atriceps* s. l. (*Formicinae*: *Camponotini*), minor and major workers, ants die biting the bark of branches, twigs, stems, exposed roots or the surface on the base of rocks, 15 Dec. 2020, *C.E. Ballesteros-Aguirre* 1247 (SC173) (**holotype** IBUG–15429; GenBank 18S: PV745542, *TEF1*: PV759188) (see Tables S1 & S2 for additional information). **Paratypes**, idem., *C.E. Ballesteros-Aguirre* 127 (SC127), 129, 132, 1210, 1231, 1242 (SC169), 1272, 1315, 1316, 1317, 1318 (IBUG) (see Table S1 for specimen information).

External mycelium scant to abundant, sometimes covering the host, initially white, gradually turning pale brown or reddish; emerges from the ant’s intersegmental membranes, concentrated on the ventral area of the host and the mandibles, adhering to the substrate. *Stroma* solitary, cylindrical to thread-like, base broadened, gradually tapering towards apex, unbranched, may fork near base or form new branches when apex is damaged, hirsute at base and towards perithecial cushion, slightly velvety towards apex, pale brown to dark brown, purple towards apex, (6.57–)9.8–17 mm long, 250–520 µm wide at base, 80–130 µm wide at apex, emerges dorsally between the head and dorsal pronotum of the ant. *Perithecial cushions* 1–4 (or more), hemispherical to ovoid, rough at maturity due to prominent perithecial ostioles, black, some lighter, 0.75–1.56 × 0.67–1.73 mm, emerge unilaterally in various places on the stroma; sometimes two perithecial cushions emerge side by side, giving the appearance of completely surrounding the stroma. *Perithecia* sub-immersed, broadly lageniform, 216–440 × 120–260 µm, neck short, perpendicular to the surface of the stroma. *Asci* cylindrical to clavate, base thinned, hyaline, (96–)106–218 × 4–10 µm, apical region 2–8.5(–18) × 3–6 µm, with 8 ascospores. *Ascospores* filiform, curved to sigmoidal, rarely straight, ends sharp, with (5–)7(–8) septa, thin-walled, hyaline, (68–)81.6–146 × 2–2.5 µm.

Ascospore germination: 1–4 capilliconidiophores, thread-like, straight, 21.5–36.5(–49) × 1 µm; with a single capilliconidium, allantoid, narrowing apically, smooth-walled, hyaline, mucus not observed, 7.5–9.5 × 2 µm.

Asexual morphs: *Hirsutella* types A and C on the same hymenium, in main stroma. *Hirsutella* type A at the apex of the stroma. *Phialides* lageniform or cylindrical, hyaline, base 3.2–10.5 × 1.6–5(–6) µm, with or without neck, (2.4–)4.8–11.5 × 0.8–1.6 µm. *Conidia* fusiform, some apiculate, hyaline, 5.5–8.5 × 2.4–3.2 µm, emerge from the neck and sometimes from the base of phialides. *Hirsutella* type C observed exclusively at early stages of development, on the base of the stroma, also forming brown sporodochia that emerge from intersegmental membranes of antennae, legs, and other body parts of ants. *Phialides* narrowly lageniform, some sub-cylindrical, gradually tapering into a long neck, cylindrical, flexuous, hyaline, base 16.5–19.5(–26) × 4–5.5 µm, neck (14.5–)17.5–23 × 1.5–2 µm. *Conidia* cylindrical to narrowly spindle-shaped, without apicule, apex rounded, base truncate, hyaline, with mucus before staining, (9.5–)10–14 × 2–2.5 µm, emerge from the neck of the phialides.

Distribution: Only known from west of Jalisco state, Mexico.

Habitat and ecology: Tropical forests, large epizootics in GF and TMCF; scattered individuals found throughout the graveyards of other species of zombie-ant fungi in SDTF. Host an undescribed species of the *Camponotus atriceps* complex, here named *Camponotus* sp. 4. Ants die biting the bark on thick branches and twigs, wrapping their legs around the twig, as well as on stems, bases, and exposed roots of trees and shrubs, sometimes at the base of rocks. Common to find specimens close to the forest floor, covered in sediments and with only the stroma visible. Stromata with positive geotropism only in branches. Zombie-ant fungi closest to the forest floor at a height of 2–5(–10) cm and the farthest at a height of 1.9–2.4(–3.5) m (n = 5 ant graveyards).

Ophiocordyceps jaliscana C.E. Ballesteros-Aguirre, L. Guzmán-Dávalos & T. Sanjuan, ***sp. nov.*** MB 859583. Fig. 8.

Etymology: Named after the Mexican state in which it was collected.

Typus: **Mexico**, west of Jalisco state, road to Haravéri Botanical Garden, 20°45’48.3”N, 104°57’14.6”W, 857 m.a.s.l., subdeciduous tropical forest, host *Colobopsis* sp. (*Formicinae*: *Camponotini*), minor workers, ants die biting the bark on stems, branches or base of bushes or trees, 24 Oct. 2020, *C.E. Ballesteros-Aguirre* 1220 (SC234) (**holotype** IBUG–15430; GenBank 18S: PV745544, *TEF1*: PV759190, *RPB1*: PV759227, *RPB2*: PV759206) (see Tables S1 & S2 for additional information). **Paratypes**, idem., *C.E. Ballesteros-Aguirre* 1154 (SC332), 1214, 1255, 1268 (SC237), 1269 (SC233), 1271, 1288, 1301 (SC330), 1302 (SC331), 1319, 1320, 1321 (IBUG) (see Table S1 for specimen information).

External mycelium scant to abundant, sometimes covering the host, initially white, gradually turning pale brown or reddish; emerges from the ant’s intersegmental membranes, concentrated on the ventral area and the mandibles of the host, adhering to the substrate. *Stroma* solitary, sub-cylindrical, cylindrical or filiform, base broadened, gradually tapering towards apex, unbranched, sometimes bifurcating near base or with new branches when apex is damaged, hirsute at the base and towards the perithecial cushion, slightly velutinous towards the apex, dark brown to purple towards the apex, pale brown with age, 4.5–10.5 mm long, 152–271 µm wide at base, 121–200 µm wide at apex, grows dorsally between head and dorsal pronotum. *Perithecial cushions* 1–2(–3), hemispherical to ovoid, rough at maturity due to prominent perithecial ostioles, brown to black, 0.66–0.78 × 0.55–0.75 mm, sometimes two perithecial cushions emerge side by side, giving the appearance of completely surrounding the stroma. *Perithecia* sub-immersed, lageniform, 204–277 × 91–122 µm, neck short, perpendicular to the surface of the stroma. *Asci* cylindrical, base thinned, hyaline, 92–135.4 × 5.5–8.8 µm, apical region 4–6 × 5.5–7.5 µm, with 8 ascospores. *Ascospores* fusoid-elongated, curved to sigmoidal, rarely straight, ends sharp, with 5 septa, thin-walled, hyaline, 63–112 × 2–2.5(–3.5) µm.

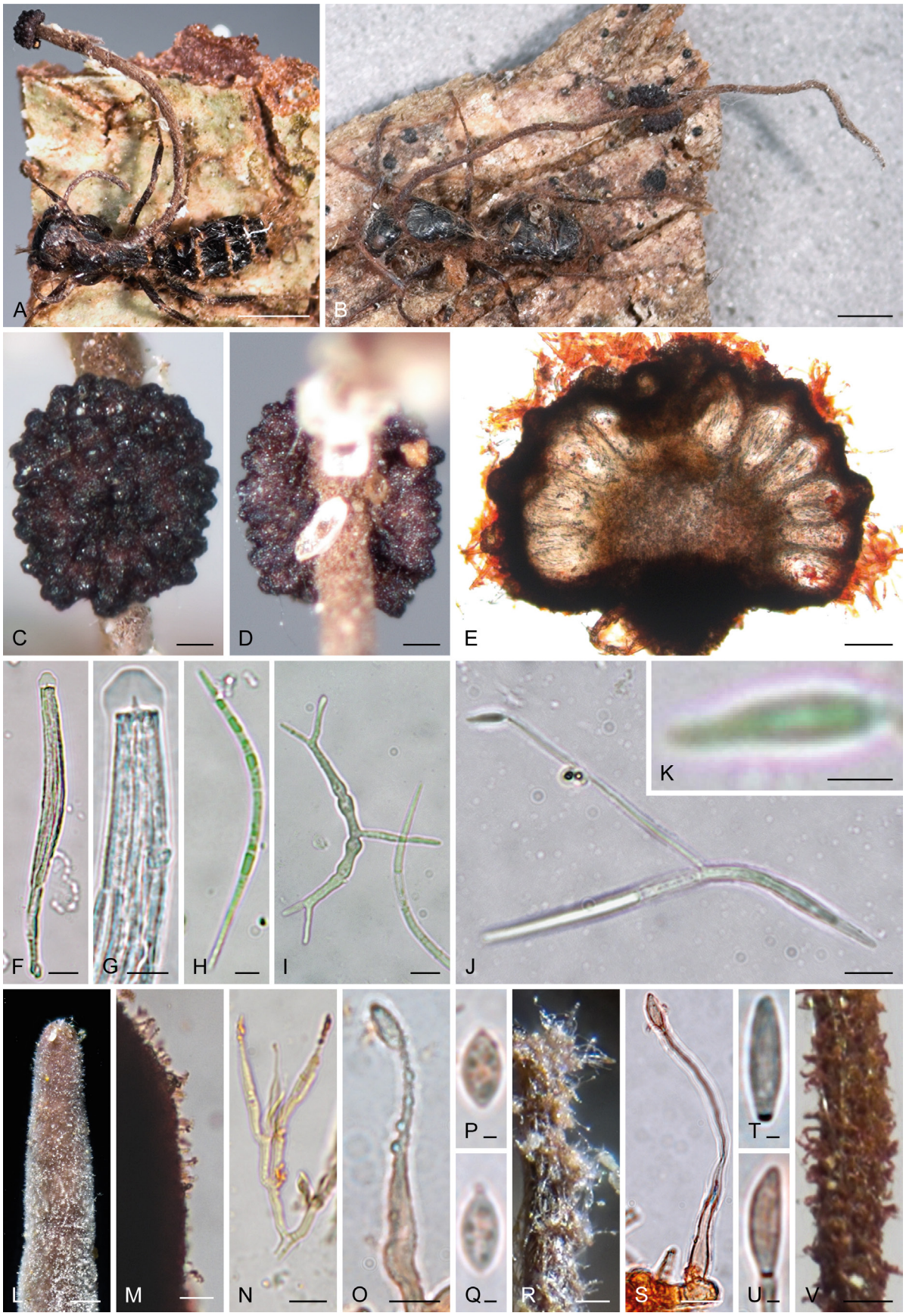

Fig. 8. *Ophiocordyceps jaliscana* (A, C–H, L–V: C.E. Ballesteros-Aguirre 1220 (SC234), holotype; B: C.E. Ballesteros-Aguirre 1154 (SC332); I–K: C.E. Ballesteros-Aguirre 1321). **A.** Hosts *Colobopsis* sp. and **B.** *Camponotus* sp. 3 (*Camp. tepicanus* s. l.), both biting the bark of a trunk with a stroma emerging between the pronotum and head, with a perithecial cushion. **C, D.** Unilateral perithecial cushion produced from the stroma. **E.** Cross-section of the perithecial cushion showing the perithecial arrangement. **F.** Ascus. **G.** Apical region of the ascus. **H.** Ascospore with five septa. **I.** Ascospore germinating in a somatic hypha, one week after being released exhibiting swollen areas. **J.** Ascospore germinating one week after being released in a capilliconidiophore. **K.** Close-up of a capilliconidium. **L–Q.** Asexual morph *Hirsutella* type A. **L, M.** Apex of a developing stroma. **N.** Phialides. **O.** Phialide with conidium. **P, Q.** Conidia. **R–U.** Asexual morph *Hirsutella* type C. **R.** Phialides. **S.** Phialide with conidum. **T, U.** Conidia. **V.** Stromal base with age. Scale bars: A–B = 1 mm; C–E, L, R, V = 100 µm; M = 25 µm; F, I, J, N, S = 10 µm; G, H, O = 5 µm; K = 2.5 µm; P, Q, T, U = 1 µm.

Fig. 9. *Ophiocordyceps pseudocamponoti-atricipis* (A–F, H, J, N–Q, S, T: C.E. Ballesteros-Aguirre 1246 (SC172), holotype; G: C.E. Ballesteros-Aguirre 131; I: C.E. Ballesteros-Aguirre 125; K: C.E. Ballesteros-Aguirre 1311; L, M: C.E. Ballesteros-Aguirre 1313; R, U: C.E. Ballesteros-Aguirre 397). **A.** Host *Camponotus* sp. 4 (*Camp. atriceps* s. l.) biting a leaf with a stroma emerging between the pronotum and head, with four perithecial cushions. **B–D.** Unilateral perithecial cushions produced on the stroma, in **B.** with three cushions. **E.** Cross-section of perithecial cushion showing the perithecial arrangement. **F, G.** Asci. **H, I.** Apical region of the asci, **I.** stained with Congo red. **J, K.** Ascospores with five septa, **K.** released on a slide inside a humid chamber. **L.** Ascospore germinating in a capilliconidiophore one week after being released. **M.** Close-up of the capilliconidium. **N.** Stromal base. **O–U.** Asexual morph *Hirsutella* type A. **O, P.** Stromal apex before and after being stained. **Q.** Phialides *Hirsutella* type A with conidia. **R, S.** Phialides stained with phloxine B. **T, U.** Conidia. Scale bars: A = 1 mm; B = 500 µm; C–E, N = 100 µm; O, P = 50 µm; F, G, J–L = 10 µm; H–I, M, Q–S = 2.5 µm; T, U = 1 µm.

Ascospore germination: Somatic hyphae or one capilliconidiophore, thread-like, straight, 52–67.5 × 1 µm; with a single capilliconidium, allantoid, narrowing apically, smooth-walled, hyaline, 7–11.5 × 1.5–3 µm.

Asexual morphs: *Hirsutella type A* on the apex of the stroma. *Conidiophores* variable, branched at different lengths, emerge directly from the stromal hyphae. *Phialides* lageniform, hyaline, base 7–14.5 × 2.5–3(–3.5) µm, flexuous neck, 3.5–14 × (0.5–)0.7–1 µm. *Conidia* widely fusiform, some apiculate, hyaline, 5.5–8.5 × (2.5–)3–3.2(–3.5) µm, emerge from the neck of phialides. *Hirsutella type C* forming brown sporodochia, emerging from intersegmental membranes of antennae, legs, other body parts of ants. *Phialides* lageniform, some sub-cylindrical, gradually tapering into a long neck, cylindrical, flexuous, hyaline, base 5.5–15(–25) × 2.5–6 µm, neck 21.3–62.5 × (1.3–)1.5 µm. *Conidia* cylindrical to narrowly spindle-shaped, without apicule, apex rounded, base truncate, hyaline, without mucus, 7–13.5 × 2.5–3 µm, emerge from the neck of the phialides.

Distribution: Only known from west of Jalisco state, Mexico.

Habitat and ecology: Tropical forests, small epizootics mainly in SDTF and TMCF, but also one graveyard was found in GF. Hosts two undescribed species: *Camponotus tepicanus* s. l., here named *Camponotus* sp. 3, and *Colobopsis* sp. Ants die biting the bark, on branches, twigs, stems, bases, and on exposed roots of trees and shrubs, even non-woody stems. It is common to find individuals covered in a very fine sediment, including the stroma. Zombie-ant fungi closest to the forest floor at a height of 2-20(–43) cm and the farthest at a height of 1.8–2.15(–2.4) m (n = 8 ant graveyards, 3 of *Camponotus* sp. 3 and 5 of *Colobopsis*).

Ophiocordyceps pseudocamponoti-atricipis C.E. Ballesteros-Aguirre, T. Sanjuan & L. Guzmán-Dávalos, ***sp. nov.*** MB 859584. Fig. 9.

Etymology: The specific epithet indicates its similarity to the species *O. camponoti-atricipis* and that it is found on *Camponotus atriceps* s. l.

Typus: **Mexico**, west of Jalisco state, Haravéri Botanical Garden, 20°45'28.2"N, 104°58'8.8"W, 754 m.a.s.l., tropical montane cloud forest, host *Camponotus atriceps* s. l. (*Formicinae*: *Camponotini*), minor and major workers, ants die on the underside of leaves, biting the ribs or margin of the leaves, 15 Dec. 2020, *C.E. Ballesteros-Aguirre* 1246 (SC172) (**holotype** IBUG–15431; GenBank 18S: PV745553, *TEF1*: PV759195, *RPB2*: 759209) (see Tables S1 & S2 for additional information). **Paratypes**, idem., *C.E. Ballesteros-Aguirre* 125, 126, 128, 130 (SC128), 131, 133, 134, 135, 136, 137, 138, 139, 140 (SC125), 141, 142, 397, 1048, 1052, 1059, 1212 (SC154), 1245 (SC171), 1278, 1293, 1311, 1312, 1313, 1314 (IBUG) (see Table S1 for specimen information).

External mycelium scant, sometimes covering the host, initially white, gradually turning pale brown; emerges from the ant's intersegmental membranes, abundant on the mandible, adhering to the substrate. *Stroma* solitary, filiform, with broad base, gradually thinning towards the apex, unbranched, sometimes forked near base or with new branches or a second stroma when the apex is damaged, velutinous to tomentose at the base and towards the perithecial cushion, slightly velutinous towards the apex, pale brown to pale pink towards the apex, (6.31–)11.5–27.5 mm long, 120–300(–500) µm wide at base, 100–110 µm wide at apex, emerges dorsally between the head and dorsal pronotum of the ant. *Perithecial cushions* 1–2(–7), hemispherical or ovoid, rough at maturity due to perithecial ostioles, brown with darker perithecial ostioles, 0.95–1.54(–2) × 0.63–1.2 mm, unilaterally attached on the stroma; sometimes perithecial cushions emerge side by side, giving the appearance of completely encircling the stroma. *Perithecia* sub-immersed, broadly lageniform, neck short, (213–)240–372 × (78–)120–160(–218) µm, perpendicular to the surface of the stroma. *Asci* cylindrical to clavate, base thinned, hyaline, 98–170 × (4–)6–8(–10) µm, apical region (3–)4–4.8 × (3–)4–5 µm, with 8 ascospores. *Ascospores* filiform, curved to sigmoidal, ends sharp, with 5 septa, thin-walled, hyaline, (72.5–)80–108(–120) × (1.6–)2–2.5(–3.2) µm.

Ascospore germination: Single capilliconidiophore, thread-like, straight, (30–)58–71 × 1–1.5 µm; with a single capilliconidium, cylindrical, apex rounded, smooth-walled, hyaline, 10–11.5 × 2 µm.

Asexual morph: *Hirsutella type A* only at the apex of stromata and synnemata. *Synnemata* solitary or gregarious, filiform, 2–6 × 0.1 mm, sometimes present in the tarsi or coxae or in other parts of the body ant, especially when the host cuticle is damaged. *Phialides* lageniform to cylindrical, hyaline, base (3.5–)4–6.5(–8) × 2.5–4(–5) µm, neck long, (4–)8–15(–17) × 0.5–1(–1.5) µm. *Conidia* widely fusiform, some apiculated, hyaline, (2.5–)3.5–5.5(–6.5) × 1.5–2.5(–3) µm, emerge at the apex of the phialides.

Distribution: Only known from west of Jalisco state, Mexico.

Habitat and ecology: Tropical forests, epizootics focused on TMCF and GF. Host an undescribed species of the *Camponotus atriceps* complex, here named *Camponotus* sp. 4. Ants die biting the main veins and leaf margins of diverse species of plants, dicots (trees and shrubs) and monocots such as bamboo. Stromata with positive geotropism. Zombie-ant fungi closest to the forest floor at a height of 20–60 cm and the farthest at a height of 0.85–1.8(–2.4) m (n = 5 ant graveyards).

DISCUSSION

The topology of the phylogenetic tree obtained in this study was consistent with previous studies (Araújo *et al.* 2018, Loreto *et al.* 2018, Wei *et al.* 2020, Tang *et al.* 2023a, b, c) and supported the hypothesis that the *Ophiocordyceps unilateralis* complex has a high specificity for ants of the *Camponotini* tribe (*Formicinae*). However, we found species in the *O. unilateralis* complex infecting turtle ants of the genus *Cephalotes* (*Myrmicinae*). This new host association changes the well-accepted paradigm that the *O. unilateralis* complex was a specific parasite of *Camponotini* ants (Evans *et al.* 2011a, Araújo *et al.* 2018). The association with

Cephalotes ants had never been mentioned before, since Tulasne & Tulasne (1865) described the first species in the *O. unilateralis* complex. On the other hand, in addition to the common ratio of one fungus to one ant (1:1) (Evans *et al.* 2011a, Araújo *et al.* 2018), we corroborated host associations of two fungi with one ant (2:1), or one fungus with two ants (1:2) (Kobmoo *et al.* 2019, Lin *et al.* 2020).

We recovered the *O. unilateralis* complex with the two major subclades already recovered by previous authors (e.g., Araújo *et al.* 2018, Tang *et al.* 2023a, b, c), subclade 1 with mostly American species, except for *O. pulvinata* from Japan and *O. tianshanensis* from China, and subclade 2 mainly with Asian species, and with *O. naomipierceae* from Australia and one unidentified species of the *O. unilateralis* complex from Ghana, Africa (Fig. 3). Our specimens were grouped in subclade 1, clustered in six clades, corresponding to six new taxa. The Mexican species were related to species from Brazil, Colombia, and the USA (Fig. 3).

Six new species of zombie-ant fungi in Mexico supported by molecular phylogeny, morphology and ecological characters

Of all the characters used to study the *Ophiocordyceps unilateralis* complex, DNA sequences employed in phylogenetic analyses and the different traits of the ascospores were the most significant for segregating the new species. However, additional characters were useful to distinguish them, such as the morphology of the asexual morphs, the species of the ants they parasitize, the positions in which the ants die (death grips), and the geographical distribution, as recommended by previous authors (e.g., Evans *et al*. 2011a, Araújo *et al*. 2018).

The myrmecophilous Mexican species have ascospores with a similar or smaller number of septa compared to the Amazonian species. *Ophiocordyceps camponoti-striati* is the sister species of *O. haraveriensis*; both have the highest number of septa compared to the other species described in this work. *Ophiocordyceps camponoti-striati* has ascospores with 12–21 septa, which makes it different from most species in the *O. unilateralis* complex, and *O. haraveriensis* with seven septa, while *O. cephalotiphila*, *O. deltoroi*, *O. jaliscana*, and *O. pseudocamponoti-atricipis* have ascospores mainly with five septa. This trait, ascospores with less than seven septa, could be considered as a synapomorphy of the clade formed by *O. cephalotiphila*, *O. deltoroi*, and *O. jaliscana*. Evans *et al*. (2011a) reported a high number of septa in the ascospores of *O. camponoti-balzani* (14–22 septa), similar to that presented in *O. camponoti-striati*, and even more in *O. camponoti-melanotici* (27–35 septa); however, in these Brazilian species the ascospores are broadly cylindrical and larger (Evans *et al*. 2011a) (Table 2). Only *O. camponoti-balzani* was included in the phylogeny and it turned out not to be closely related to *O. camponoti-striati*.

Ophiocordyceps jaliscana is the sister species of the clade formed by *O. cephalotiphila* and *O. deltoroi*. The three species produce similar ascospores and *Hirsutella* types A and C asexual morphs. However, *O. deltoroi* has bigger stromata and perithecial cushions. *Ophiocordyceps deltoroi* and *O. cephalotiphila* are different from *O. jaliscana* due to the presence of multiple asexual stromata emerging from various parts of the ant. Regarding the host, *O. jaliscana* is associated with two different ants, *Camponotus tepicanus* s. l. and an undescribed species of *Colobopsis*, sharing a single host with *O. deltoroi: Camp. tepicanus* s. l.; however, the morphology of the sexual and asexual morph forms differs between the two species. When *O. deltoroi* parasitizes *Camp. tepicanus* s. l. it produces only asexual stromata, in contrast, *O. jaliscana* produces holomorphic stromata in this ant species. The extended phenotype also differs, *O. cephalotiphila* and *O. jaliscana* force ants to die by biting only vegetation while *O. deltoroi* forces ants to die on both vegetation and rocks. Another distinctive feature of *O. deltoroi* is that it produces large epizootics in TMCF.

Ophiocordyceps deltoroi and its sister species *O. cephalotiphila* produce similar ascospores, capilliconidiophores, and *Hirsutella* types A and C asexual morphs. However, *O. deltoroi* is distinguished by the presence of stromata on the sides of the host mesonotum, as well as larger stromata and perithecial cushions. *Ophiocordyceps cephalotiphila*, on the other hand, has no stromata on the sides of the mesonotum and smaller stromata and perithecial cushions. The hosts, behavior manipulation mode, and the habitat are also different because *O. deltoroi* parasitizes *Camponotus sericeiventris* s. l. and *Camp. tepicanus* s. l. on the base of trees and rocks and produce epizootics in TMCF, while *O. cephalotiphila* parasitizes *Cephalotes* ants in the base of the trees and produce epizootics in SDTF.

Ophiocordyceps deltoroi is the most similar to *O. unilateralis* s. str., as both exhibit similar stromata, *Hirsutella* types A and C asexual morphs in the same hymenium of the stromata, produce independent synnemata, and sporodochia with type C phialides on the legs or other parts of the ant ‘s body. However, *O. unilateralis* s. str. differs in the smaller asci, (90–)95–125 × 6–8 (–9) µm, shorter ascospores, (70–)75–85 µm (Table 2), and non-apiculate conidia type A, only emerging from the neck of the phialides. Besides, in the extended phenotype in *O. unilateralis* s. str. the host *Camponotus sericeiventris* s. l. die biting the leaves on bushes (Evans *et al.* 2011a), meanwhile *O. deltoroi* hosts die biting trees and rocks. Finally, the habitat and distribution of *O. unilateralis* s. str. is the Atlantic rainforest in Brazil (Evans *et al.* 2018).

In contrast, the asexual morphs of *O. deltoroi* correlate with an undescribed species of the *O. unilateralis* complex from Honduras, mentioned by Evans & Samson (1984) as *Hirsutella formicarum* Petch. They match in the shape of the stromata with ramifications, shape and colour of the perithecial cushions, presence of independent synnemata in the host appendages, *Hirsutella* types A and C on the stroma [type C as *Hirsutella* type B in *H. formicarum* sensu Evans & Samson (1984), or as *Hirsutella* type C in *H. sporodochialis* sensu Evans *et al.* (2011a)] (see Fig. 2) asexual morphs, shape and colour of the phialides, apiculate conidia type A, and in the size, shape, colour, and presence of mucus in the type C conidia. In the Honduran species, the host is a species of the *Camp. sericeiventris* complex and the ants die biting on the base of the trees in tropical forest. It slightly differs in the size of the conidia type A, 3–6 µm long. The presence of sporodochia in antennae and legs was not mentioned for *H. formicarum*, nor were asci or ascospores described. Future analyses are required to establish the identity and phylogenetic relationship of the Honduran species.

Ophiocordyceps haraveriensis shares macromorphology

with *O. kimflemingiae*, as both species have similar stromata, perithecial cushions, and extended phenotype, but are phylogenetically distant and ecologically different. *Ophiocordyceps kimflemingiae* always manipulates the ants to die biting on twigs and develops stromata with positive geotropism. On the other hand, *O. haraveriensis* kills ants biting not only the bark but also rocks, and although it also develops stromata with positive geotropism, this feature is restricted to those biting on the twigs, in other substrates as the stems, base of plants, and rocks the positions are variable. Furthermore, *O. kimflemingiae* has wider asci, 10–11 µm in diameter, wider ascospores, 5 µm diam., with 5–6 septa, and longer capilliconidiophores, 80–100 µm (Table 2). In addition, differences in habitat (temperate deciduous forest) reflect variants in the extended phenotype, as *O. kimflemingiae* causes *Camponotus castaneus* to die by biting twigs and wrapping its legs around them, giving additional support to the fungus (Araújo *et al.* 2018, Loreto *et al.* 2018).

The Mexican species *O. pseudocamponoti-atricipis* is the sister species of the Amazonian *O. camponoti-atricipis*, but this relationship was poorly supported (Fig. 3). Both are morphologically similar, but the latter has shorter asci, 110–140 µm and shorter ascospores, (75–)80–85(–100) µm (Araújo *et al.* 2015) (Table 2). These fungi are associated with two different ants within the *Camponotus atriceps* complex, and, in turn, with different distribution ranges (Mackay 2019, Bolton 2024). Also, the death grips are slightly different; in *O. camponoti-atricipis* the ants are commonly found biting the apical part of palm-fronds, dicot leaves, and rarely on palm-spines; instead, ants infected by *O. pseudocamponoti-atricipis* die on the underside of various types of dicotyledons and monocots, similar to some Thai species, e.g., *O. camponoti-leonardi*. Kobmoo *et al.* (2012, 2019) revealed the existence of the cryptic species, *O. camponoti-leonardi*, *O. camponoti-saundersi*, and *O. polyrhachis-furcata*, genetically differentiated and with different distribution, very similar at a macromorphological level to the species described here. Based on all the aforementioned, its different morphology, distribution, and host become relevant to sustain *O. pseudocamponoti-atricipis* as a new taxon. In addition, *O. pseudocamponoti-atricipis* shares the host within the same habitat, even the same plants with *O. haraveriensis,* but the morphology of the fungi, the position in which the ant dies, and their phylogenetic position clearly distinguish both species.

We did not find notable differences among the capilliconidia of the new species in which we managed the ascospore germination. However, *O. haraveriensis* produced capilliconidiophores relatively shorter, approx. 20–35 µm long, which are a quarter part of the total length of the ascospores, approx. 80–140 µm long. Descriptions of similar capilliconidiophores were made for *O. camponoti-novogranadensis* and *O. camponoti-sexguttati* (Evans *et al.* 2011a, Araújo *et al.* 2018). The ascospores of *O. cephalotiphila*, *O. jaliscana*, and *O. pseudocamponoti-atricipis* showed similar shape, size, and germination, with the ascospores approx. 63−110 µm long and the capilliconidia approx. 37–79 *µm* long. Nevertheless, these similarities are homoplasies because the species belong to different clades.

Araújo *et al.* (2018) hypothesized that the size and shape of the capilliconidiophores could be the result of a local adaptation between the pathogen and the morphology/ecology of the ants, due to the correlation they found between the long capilliconidiophores exhibited in *O. camponoti-indiani* and the large size of the host, *Camponotus indianus* (Araújo *et al*. 2015). In our case, we could not find this correlation in the Mexican species, since, for example, the shorter capilliconidiophores of *O. haraveriensis* did not correlate with the size of its host, *Camp. atriceps* s. l., which is relatively larger than other parasitized ants studied.

A particular feature was observed in *O. jaliscana*, where most of the germinated ascospores produced somatic hyphae with swollen areas. A similar behaviour has only been reported in *O. kimflemingiae* and *O. satoi* from South Carolina (USA) and Japan, respectively, both in temperate forests. Araújo *et al.* (2018) hypothesized that this trait might be related to adaptations to those habitats. However, we found the same type of germination in different samples of *O. jaliscana* in humid (TMCF) and sub-deciduous tropical forests (SDTF). Future studies in Mexico could test whether there is a correlation between germination into somatic hyphae and the type of forest.

In our work, we found that five of the new species here described have *Hirsutella* types A and C (see Table 2), except for *O. pseudocamponoti-atricipis* with only type A. The species of the *O. unilateralis* complex present four types of hirsutelloid asexual morphs: A, B, C, and one similar to *Paraisaria* (*O. naomipierceae*), which differ in shape and ecological function (Evans *et al*. 2011a, b, Araújo *et al*. 2018). The hirsutelloid asexual morphs in Mexican species are present from early stages of the stromata until the last moments of the fungus, when only a few remnants of the ant's body persist. The presence of *Hirsutella* type C on the surface of perithecial cushions of the fungus and external mycelium had not been reported for any species of the complex, and here we report it in *O. cephalotiphila*.

Hosts

Ants of the genera *Camponotus*, *Colobopsis*, *Dinomyrmex*, and *Polyrhachis* (*Camponotini*) have been recorded as the hosts of the *O. unilateralis* complex after more than 150 years of studies with specimens from Africa (Ghana), America (Brazil, Canada, Colombia, Costa Rica, Guyana, Ecuador, Honduras, Nicaragua, north and east of the USA, Panama, Peru, and Venezuela), Asia (China, Japan, Indomalaya region, and Taiwan), and Australia (Tulasne and Tulasne 1865, Evans & Samson 1984, Sanjuan *et al.* 2001, Evans *et al.* 2011a, Kepler *et al.* 2011, Araújo *et al.* 2015, 2018, Loreto *et al.* 2018, Lin *et al*. 2020, Tang *et al*. 2023a, b, c). Specifically, Loreto *et al.* (2018) mentioned that species of this complex were present in 26 countries and made evident the lack of records in Mexico. We hypothesized, from personal observations and unpublished records, that there are many undescribed species of the *O. unilateralis* complex in Mexico, not only in *Camponotini*, but also in *Myrmicinae* ants, i.e., *Cephalotes*, as those illustrated in Fig. 10, from Chiapas, Jalisco, and Quintana Roo, Mexico.

Furthermore, we discovered that two zombie-ant fungi can sympatrically parasitize one species of host and the existence of zombie-ant fungi specialized in two different hosts (Fig. 3). Similar results had been reported by Kobmoo *et al.* (2019), Lin *et al.* (2020), and Tang *et al.* (2023a, b, c). In this work, we tested the different hosts associations considering the morphology of the fungi on different samples,

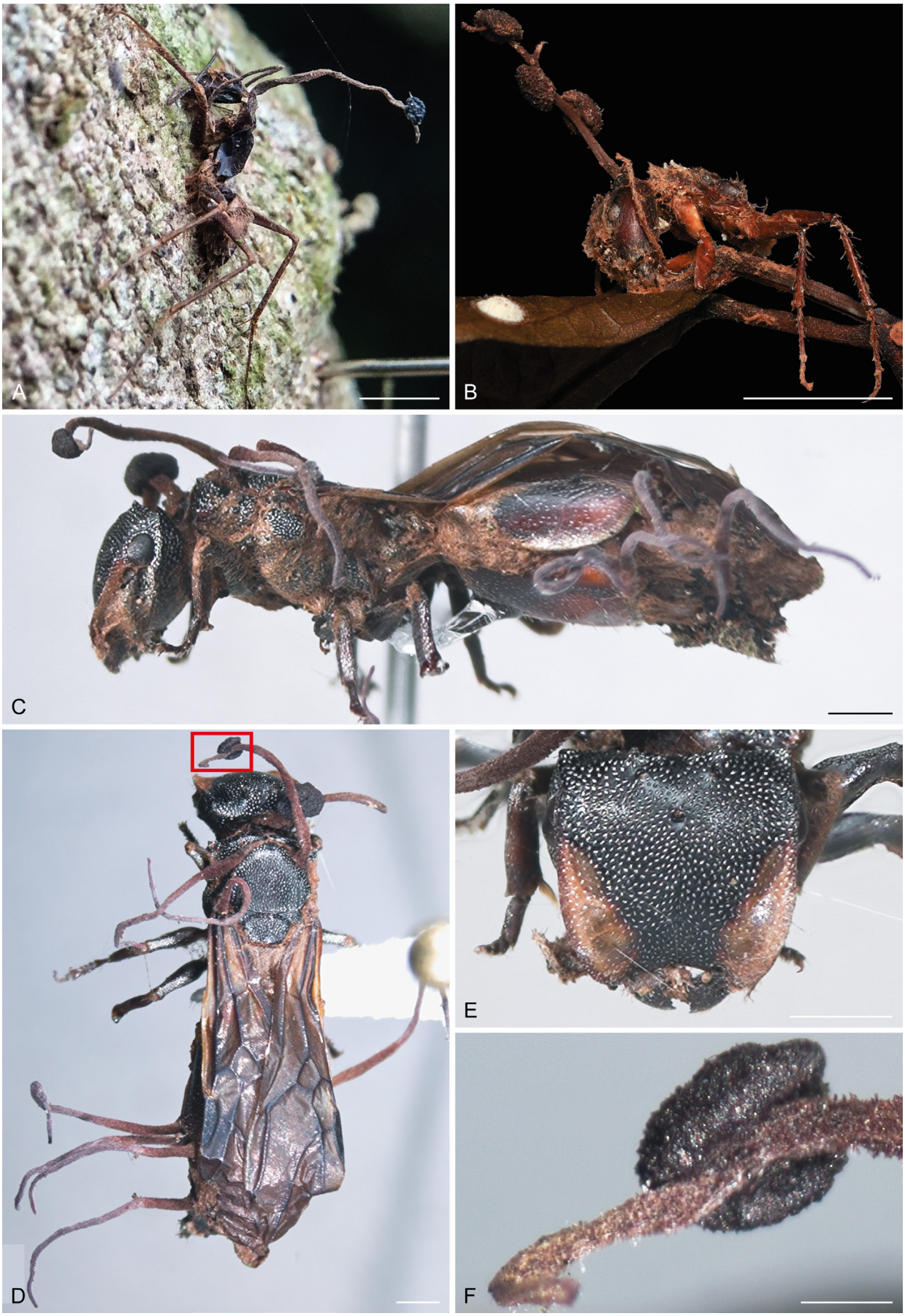

Fig. 10. Ants parasitized by an undetermined species of the *Ophiocordyceps unilateralis* complex from other regions in Mexico. **A.** *Camponotus* sp. manipulated to die biting bark from the study site. **B.** *Camponotus atriceps* s. l. biting the petiole of a leaf from Quintana Roo (photo credit: Leon Esteban Ibarra Garibay, 2 May 2022). **C–F.** Specimen collected in Chiapas. **C.** Winged gyne of *Cephalotes* sp. mounted in a pin, found in the field biting the bark of a trunk, with the main stroma behind the head and other stromata emerging on the mesosoma, gaster, and legs of the ant. **D.** Dorsal view of the host and stromata. **E.** Frontal view of the host's head. **F.** Immature unilateral perithecial cushion produced from the stroma, close-up of the red rectangle in D. The three specimens with holomorphic stroma between head and pronotum, the mycelium under the ant gaster and legs adhere to the bark and keep the fungus fixed. Scale bars: A–B = 5 mm; C–E = 1 mm; F = 250 µm.

especially those that share a host in the same graveyards.

In determining the host species, it must be considered that some *Camponotus* belong to species complexes (Mackay 2019). That is, these ants belong to hyperdiverse groups that, unfortunately, to date, do not have a solid taxonomic and systematics foundation. We assumed that the *Camponotus* species associated with the zombie-ant fungi described above are different from those present in Brazil, which are hosts of *O. camponoti-atricipis* and *O. unilateralis* s. str. (Evans *et al.* 2011a, 2018, Araújo *et al.* 2015). Kobmoo *et al.* (2019) noted that the hosts of *O. camponoti-leonardi* and *O. camponoti-saundersi*, the ants *Colobopsis leonardi* and *Colo. saundersi*, were also species complexes. Therefore, associations of one fungus with different hosts, or two species of fungi with two hosts may exist in different places. The determination of ants can be complemented by phylogenetic analysis employing DNA sequences, which is useful to show more precisely the identity of the hosts associated with the fungi (Tang *et al.* 2023a, b, c).

We corroborate the species of the different hosts with morphology and phylogenetic analyses employing *COI* sequences; the results showed (not presented here) that there are different species of *Camponotus*, *Cephalotes*, and *Colobopsis*. Tang *et al.* (2023a, b, c) employed the same DNA locus to demonstrate the associations of three species of the *O. unilateralis* complex with species of *Camponotus*, *Colobopsis*, and *Polyrhachis*. Ballesteros-Aguirre *et al.* (unpublished) inferred the phylogenetic relationships of the ants and found the existence of a new species of *Colobopsis*, which will be described, supported by the specific association with *O. jaliscana*.

In our sampling, we noted that different ant castes were susceptible to parasitism by the *O. unilateralis* complex. The workers, major workers (soldiers), and even queens were infected and exhibited the extended phenotype and stromata of the fungi. Similar results were reported for *O. corriemoreauae*, a myrmecophilous hymenostilboid fungus, which can infect workers, gynes, and males (Araújo *et al.* 2020). It is likely that zombie-ant fungi can parasitize all castes of ants. However, in our results, we did not find males parasitized by the fungi, nor did we find any other report that fungi of the *O. unilateralis* complex parasitized males. In the case of *O. jaliscana*, we only collected infected minor workers of *Colobopsis*, even though five graveyards were sampled. Nevertheless, further sampling is recommended to confirm whether these zombie-ant fungi specialize in this particular caste of ants.

We confirm that the ant nests are very close to the zombie-ant fungi graveyards, unlike what was previously observed by Pontoppidan *et al.* (2009), with species of the *O. unilateralis* complex from Thailand. The species of *Camponotus*, *Cephalotes*, and *Colobopsis* used only rotten wood for nesting. The small ant species, such as *Camp. striatus*, *Camp. tepicanus*, and *Colobopsis* sp., tend to nest in hollow twigs. The bigger ants, such as *Camp. atriceps* and *Camp. sericeiventris*, tend to nest in hollow logs and in living and dead trees. *Cephalotes goniodontus* and *Ceph. hirsutus* prefer hollow logs in the canopy, or even near the forest floor, or in living or dead trees. In most cases, the zombie-ant fungi graveyards were located a few meters from the nest, even on the same bush or tree. In the case of *Camp. sericeiventris*, no nests were found near the graveyards, as these ants may possibly nest in dry branches in the canopy. Most of our results contrast with Pontoppidan *et al.* (2009), as they suggested that foraging host ants actively avoid graveyards. In their results, they found that host ants built nests high in the canopy and only occasionally descended through the graveyards in search of resources on the forest floor. We observed that ants had a close relationship with graveyards, as ants were found actively foraging day and night in and around them, and it was at those moments that infection occurred. As mentioned above, in this work the taxonomic determination of the hosts is considered relevant to better understand the ecological interactions of ant-zombie fungi. Therefore, it is recommended to carry out studies that shed more light on the ecological patterns in the graveyards of the different species of zombie-ant fungi from Mexico.

Graveyards

In our study, the graveyards were composed of either one or multiple species of *O. unilateralis* complex with different host species. *Ophiocordyceps camponoti-striati* specimens were inconspicuous due to the small size of the host (~3 mm long); therefore, few individuals were found in two different graveyards, ~25 m apart. *Ophiocordyceps cephalotiphila* formed focalized epizootics mainly in SDTF, but we recorded a graveyard in GF, with a density in the tens (i.e., 10−20) to hundreds of individuals in some areas, with larger trees having a higher density. It was common to find several ants biting the bark in the same area or even ants using other infected ants as substrate (Fig. 11E−F). Similar observations were made with other zombie-ant fungi from other complexes, such as *O. kniphofioides* that forces *Cephalotes atratus* to die next to each other in the graveyards (Evans & Samson 1982, Araújo *et al.* 2018, Imirzian *et al.* 2020).

Ophiocordyceps deltoroi formed extended epizootics in TMCF, with a high density that could include hundreds of individuals in some areas. *Ophiocordyceps haraveriensis* was irregularly distributed throughout the whole study area, with few individuals in SDTF, but forming focalized epizootics in GF and TMCF, with a density that could be in the tens to hundreds of individuals in some areas. *Ophiocordyceps jaliscana* formed small epizootics in the tens (i.e., 10−20 individuals) mainly in SDTF and TMCF. *Ophiocordyceps pseudocamponoti-atricipis* formed focalized epizootics in GF and TMCF, with a low density that could be in the tens (i.e., 10−50 individuals). In contrast, Araújo *et al.* (2015) reported higher density in some areas of Amazonian forests, even multiple ants belonging to different species, biting the same leaf.

Even though the graveyards can be occupied by different species of *O. unilateralis* s. l., there is little evidence of cross-infection within overlapping or sympatric ant populations (Evans *et al.* 2011a, de Bekker *et al.* 2014, Kobmoo *et al.* 2019). Although our sampling was based on the criterion of collecting individuals according to the morphology of fungi and ants, as well as the extended phenotype observed, it was common for the new species presented here to share hosts and cemeteries in different parts of the vegetation. Therefore, experiments are needed to determine whether there is any degree of hybridization due to cross-infection.

In the case of *O. cephalotiphila*, which infected *Cephalotes goniodontus* and *Ceph. hirsutus* at the base of trees, we

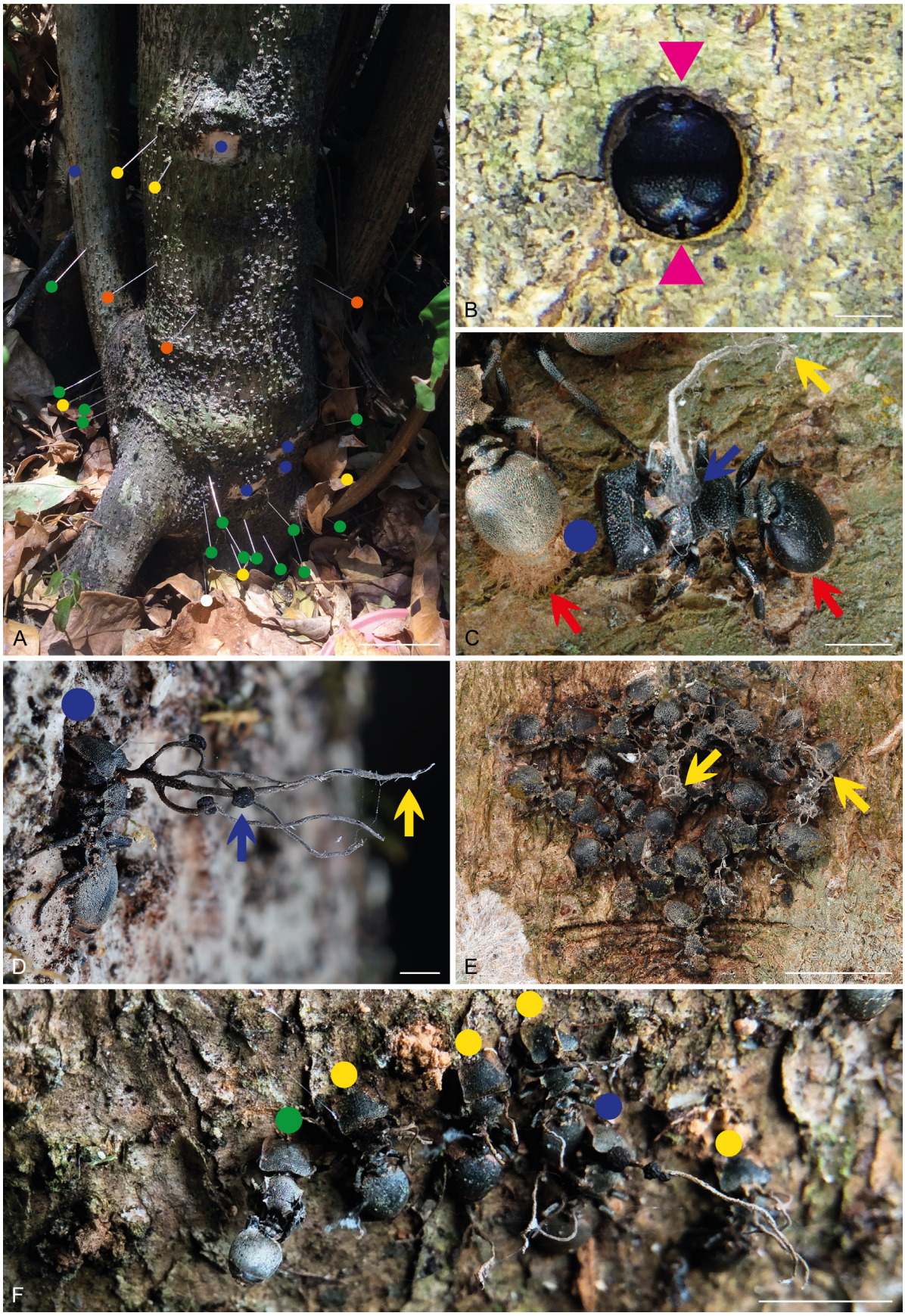

Fig. 11. Habit and extended phenotype of *Ophiocordyceps cephalotiphila*. **A.** Graveyard of *Cephalotes hirsutus* on the base of a shrub, the pins indicate the position of the zombie-ant fungi, blue: fungi with mature perithecial cushions, green: attached ants without stroma, orange: fungi with immature perithecial cushions, white: remains of the zombie-ant fungi, yellow: fungi with asexual stroma. **B.** Nest entrance blocked by two phragmotic major workers (soldiers) of *Ceph. hirsutus* (pink triangles), near the graveyard. **C.** Phragmotic major worker infected, perithecial cushion (blue arrow), asexual morph (yellow arrow), and the site where the mycelium adheres to the bark (red arrow), blue dot, see A. **D.** Major worker of *Ceph. goniodontus*, perithecial cushion (blue arrow) and asexual morph (yellow arrow) (blue dot, see A). **E.** Graveyard of *Ceph. goniodontus* and *Ceph. hirsutus*, dead together on the base of a tree, some using other infected ants as substrate (asexual morphs marked with yellow arrows). **F.** Graveyard of *Ceph. goniodontus*, fungi in different stages of development (for an explanation of the coloured dots, see A), an ant (blue dot) using another ant as a substrate. Scale bars: A = 5 cm; B–D = 1 mm; E–F = 5 mm.

found that ants died in highly aggregated distributions, suggesting that infected ants find zombie ant cadavers attractive to die alongside (Fig. 11A, E−F). *Ophiocordyceps cephalotiphila* persisted continuously in the environment with its different *Hirsutella* asexual morphs; for example, type C phialides are designed to infect by contact and persist in the exoskeletal remains of zombified ants. In contrast, Evans & Samson (1982) described that apparently uninfected *Ceph. atratus* ants take off cadavers of infected ants from the bark, suggesting a protective behavior against the fungal infection. However, the fungus *O. kniphofioides* s. str. has a strategy for persisting in the environment, expressing a characteristic asexual morph described as *Hirsutella stilbelliformis* var. *stilbelliformis*, which has a rhizoid-like outgrowth that persists in the moss carpet and bark, even if the ant is removed. This asexual structure produces synnemata with yellow conidial masses at the apex, which remain infective upon contact (Araújo *et al.* 2018). *Hirsutella* type *stilbelliformis* asexual morphs are exclusive to the *O. kniphofioides* complex (Evans & Samson 1982, Araújo *et al.* 2018).

During the rainy season, we observed ants of the *Cephalotes* genus occasionally wandering through the graveyards, and during the dry season, we witnessed ants with arboreal habits that came down to the forest floor in search of resources, and most likely, becoming infected in the graveyards. Nests have occasionally been found very close, 1−2 m from graveyards, and we think there may be more nests in the canopy, as these ants are polydomous and occupy many nests in abandoned cavities or at the ends of broken branches in dead wood (Gordon 2012, Vergara-Torres *et al.* 2016). Fungi are likely taking advantage of these ant habits to spread in the forest.

Similar ecological observations were made by Imirzian *et al.* (2020) with *Ceph. atratus* infected by *O. kniphofioides*, where it seems that some trees were used for climbing or descending more frequently, promoting the aggregation of cadavers on the base of trees (infection hotspots). Nevertheless, host behaviour differs because *Ceph. atratus* workers remove infected ants from trees, suggesting some defence against infection. Our field observations indicated that Mexican *Ophiocordyceps* constantly interact with their hosts and that there was no behaviour suggesting any type of defence by the ants, as occurs in the interaction between *O. kniphofioides* and its hosts. At the same time, being close to the host leads to a high frequency of transmission that gives rise to epizootics. Future studies may investigate the entire infection system and expose the factors that promote host-parasite coexistence.

There is an interesting behaviour in *Ceph. hirsutus*, where the head of the major workers and queens is modified as a "cork" and is used as a physical defence strategy blocking the entrance to the nest, functioning as a kind of "living door" (Creighton 1967, Powell *et al*. 2020). This adaptation is called phragmosis (Wheeler 1927, Hölldobler & Wilson 1990). We found the major workers and queens of *Ceph. hirsutus*, whose job is to guard the entrance to the burrow (Fig. 11B−C), were somehow infected and manipulated into going and dying by biting the bark at the base of trees in the graveyards. It was evident that there is an indirect infection mechanism. We hypothesize that the minor workers are responsible for dispersing these parasitic fungi at the entrance and inside the nest. It is likely that they carry some spores attached to their bodies and disperse them by contact with other ants, due to their high sociability. Microscopic observations showed that *O. cephalotiphila* produces many sticky conidia on type C phialides, which are active through the year in the graveyards, shedding light on how ants can become infected inside nests.

Extended phenotype

Our phylogenetic results suggest that in subclades 1 and 2, i.e., in the *O. unilateralis* complex, twigs and bark are the ancestral death position of ants when infected (Fig. 3). These results differ from those shown in Loreto *et al.* (2018), where the ancestral position was leaf biting, due to the addition of the new Mexican species, as well as the inclusion of *O. tianshianensis* from China (Wei *et al.* 2020) and an undescribed Ghanaian specimen of the *O. unilateralis* complex (Araujo *et al.* 2018). The results also show that the bark is the ancestral death position in *O. kniphofioides*, consequently for the hirsutelloid ant pathogen clade. In this case, the result is in agreement with Loreto *et al.* (2018) and Tang *et al.* (2023c). So far, only the Mexican species in the *O. unilateralis* complex manipulate the ants to die at the base of rocks, thus they present a unique extended phenotype. If we consider that the base of the rocks presumably maintains constant humidity, then we might think that this location provides favourable environmental conditions for the development of the fungal sporomes. The difference between extended phenotypes in the *O. unilateralis* complex could be due to adaptative plasticity in response to environmental characteristics and changes. Until now, we know the death position is a trait that has evolved convergently in different regions of the world (Loreto et al. 2018).

The common trait in five of the newly proposed taxa was biting the bark of branches or the base of trees or shrubs, but we also found zombie-ant fungi on the base of rocks and only *O. pseudocamponoti-atricipis* forced ants to die by biting the main veins or margins of leaves (Figs 11, 12). Other substrates where ants die have been reported, such as climbing stems, epiphytes, green twigs, inside logs, fallen logs, lianas, lichens, and palm thorns (Evans & Samson 1984, Kepler *et al.* 2011, Araújo *et al.* 2015, 2018, Kobmoo *et al*. 2015, Wei *et al*. 2020). It was proposed that in non-deciduous forests ants bite leaves, while they bite twigs in deciduous forests; however, extended phenotype, habitat, and even the host are homoplastic characters in the *O. unilateralis* complex (Loreto *et al.* 2018). The common extended phenotype in the tropical forests in Mexico could be to bite the bark, according to our sampling in Jalisco. So, the behaviour of biting branches or bark is not characteristic only of deciduous forests, but also exists in evergreen forests, even tropical ones.

The taxa proposed here expressed specific variation among themselves with respect to the height from the forest floor at which ants die, with a wide range from 2 cm to almost 3 m above the ground, compared to other species that kill ants on the bark. For example, *O. kimflemingiae* forced the ants *Camp. castaneus* to die biting twigs about 0.5–1.5 m from the forest floor (Araújo *et al.* 2018, Loreto *et al.* 2018). On the other hand, *O. deltoroi* manipulated its two hosts to die by biting onto bark at a different height above the forest floor (Table S1). When *O. deltoroi* parasitized *Camp. sericeiventris* s. l., the ants died at the base of trees, 2 cm to 1.55 m from the forest floor, but when *Camp. tepicanus* s. l. was parasitized, it

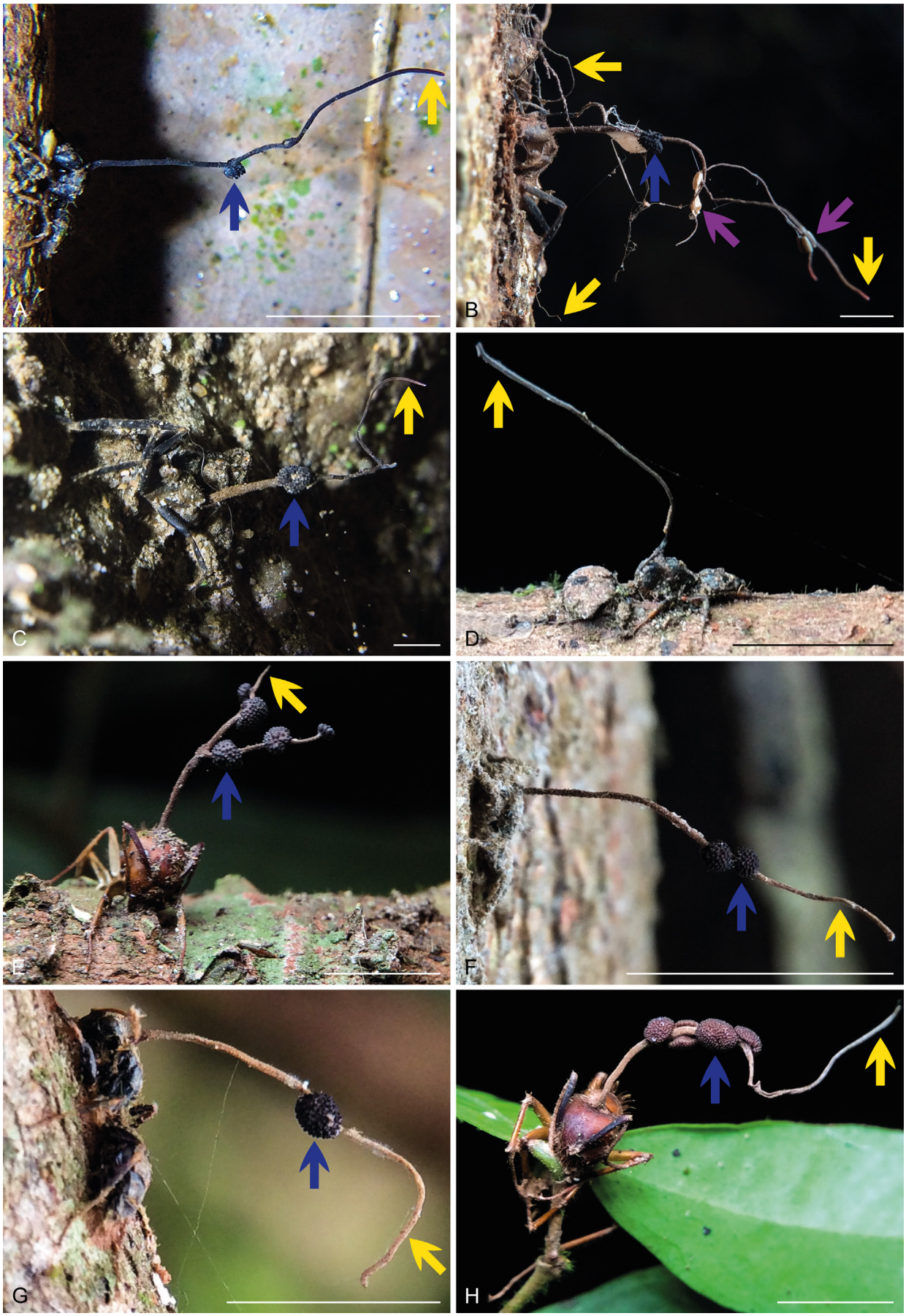

Fig. 12. Habits and extended phenotypes of the new species. Perithecial cushions (blue arrows), asexual morph areas (yellow arrows), pupa of an undetermined insect (purple arrows). **A.** *Ophiocordyceps camponoti-striati* manipulating *Camponotus striatus* s. l. to die biting bark. **B–D.** *Ophiocordyceps deltoroi*. **B.** *Camponotus sericeiventris* s. l. manipulated to die biting bark on the base of a tree. **C.** *Camponotus sericeiventris* s. l. manipulated to die biting a base of a rock, covered in sediment. **D.** *Camponotus. tepicanus* s. l. manipulated to die biting bark. **E.** *Ophiocordyceps haraveriensis* manipulating *Camp. atriceps* s. l. to die biting bark. **F, G.** *Ophiocordyceps jaliscana* manipulating its hosts to die biting bark. **F.** *Colobopsis* sp. **G.** *Camponotus tepicanus* s. l. **H.** *Ophiocordyceps pseudocamponoti-atricipis* manipulating *Camp. atriceps* s. l. to die biting a leaf. Scale bars = 5 mm.

was 4.5 cm to 2.56 m from the ground. A generalist species of the *O. unilateralis* complex, which manipulates seven species of *Polyrhachis* and one of *Camponotus* in an evergreen broad-leaf forest in central Taiwan, also uses ants to disperse in the habitat in different ways, as the height from the forest floor varies in a host-dependent manner (Lin *et al.* 2020). The different extended phenotypes of Mexican zombie-ant fungi, when ants died by biting bark, possibly reflect the way the fungi can take advantage of different niches in diverse vegetation types.

In the case of the fungi that force ants to die by biting the leaves, we found that *O. pseudocamponoti-atricipis* kills *Camp. atriceps* s. l. over a wider range of heights (20 cm to 2.4 m from the ground), compared to the sister species *O. camponoti-atricipis* from the Brazilian Amazonia, which manipulates the ants, *Camp. atriceps*, to die by biting the apical part of palm-fronds, dicot leaves, and palm-thorns, over a shorter and lower range, around 60 cm to 1.4 m above the floor level (Sanjuan *et al.* 2001, Araújo *et al.* 2015, Andriolli *et al.* 2019). Possibly the variations are caused by the influence of different plant species, as well as the intrinsic differences of each species, but additional studies are needed to more accurately describe the ecological patterns.

Loreto *et al.* (2018) suggested that the extended phenotype of the fungus is influenced by the habitat and determines the optimal site where ants bite before dying. We found two species that sympatrically parasitized the same ant species, but that expressed a different extended phenotype. *Ophiocordyceps haraveriensis* and *O. pseudocamponoti-atricipis* are fungi of different lineages that parasitize *Camp. atriceps* s. l. (*Camponotus* sp. 4) (Fig. 3); the first manipulated the ants to bite bark, twigs, and rocks, and the second to bite leaves. On the other hand, *O. deltoroi* and *O. jaliscana*, both belonging to the same lineage (Fig. 3), manipulated *Camp. tepicanus* s. l. (*Camponotus* sp. 3) to bite the bark, branches, and base of trees, but only *O. deltoroi* to bite the base of rocks. According to Loreto *et al.* (2018), ants manipulated to bite the bark of trees are not frequent. Until this work, most species of the *O. unilateralis* complex were observed to manipulate ants to bite leaves and were found in non-deciduous forests in the tropics. This extended phenotype was hypothesized to be the ancestral trait that subsequently switched to twig biting at least four times in different lineages (Loreto *et al.* 2018). However, this may need to be re-considered in the light of the evidence from Neotropical species. Twig-biting and other behaviours, such as twig-grasping, could be explained by phenotypic plasticity, which evolved convergently in different areas of the globe due to the appearance of deciduous forests (Loreto *et al.* 2018).

Both leaves and twigs are available throughout the year in the GF and TMCF, but in the SDTF the seasonality results in several plants losing their leaves. Previous studies suggested that leaves can provide a favourable microclimate, with stable temperature and humidity, as well as protection from UV rays and rain (Andersen *et al.* 2009, Pincebourde & Woods 2012). However, we found that in the three sampled tropical forests the bark could also provide a favourable microclimate, even if the fungus is not protected from UV damage and rain, although, in many cases, this protection could be provided by the canopy. In tropical forests, development of zombie-ant fungi individuals occurs within a few months, but in temperate forests development occurs within at least a year (Mongkolsamrit *et al.* 2012, Loreto *et al.* 2014, 2018, Araújo *et al.* 2015). In the case of *O. kimflemingiae*, leaf fall, lower average annual temperature, and slow development rate in the temperate forest where this species thrives, probably selectively favoured twig biting by the host (Loreto *et al.* 2018). The Mexican species belong to a different lineage within the *O. unilateralis* complex, and the tropical forest and environmental conditions are very different from those to which *O. kimflemingiae* is exposed. Therefore, the reason why Mexican species manipulate ants to bite the bark remains unknown. The answer could be found by analysing the biogeographic history of *the O. unilateralis* complex, and other taxa that share a common evolutionary history (cenochrons), in the Mexican Transition Zone, where the Neotropical and Nearctic biotas overlap (Morrone 2020), since there is a possibility that the extended phenotype of fungi is related to changes in the physiognomy of vegetation, landscape, and ant lineages. Further exploration and collections are needed to better understand the biogeographic history of the *O. unilateralis* complex throughout the Mexican territory, both in the Neotropics and the Nearctic. The discovery and description of the first species of the *O. unilateralis* complex in Mexico provides evidence that allows a better understanding of the ecological interactions of the zombie-ant fungi with their hosts.

ACKNOWLEDGEMENTS

The authors are thankful to SECIHTI (grant to CVU 1083967) and University of Guadalajara for financial support. We also thank Biol. Mónica Rivas Avendaño and all the staff of the Haravéri Botanical Garden for all the attention they provided in the logistics of the sampling that made this study possible. Special thanks to Eng. Salvador Galindo, owner and founder of the Haravéri Botanical Garden, for his support with transportation, accommodation, and food during the field work. We would like to thank Biol. Sergio Fausto for his collaboration in the germination of ascospores, Kent Brothers for English language editing and special thanks to nature enthusiast Marco Antonio Cortes Esparza for his valuable collaboration during the sampling efforts.

Declaration on conflict of interest. The authors declare that there is no conflict of interest.

REFERENCES

Aljanabi SM, Martinez I (1997). Universal and rapid salt-extraction of high quality genomic DNA for PCR-based techniques. *Nucleic Acids Research* **25**: 4692–4693. https://doi.org/10.1093/nar/25.22.4692

Altschul SF, Gish W, Miller W, *et al.* (1990). Basic local alignment search tool. *Journal of Molecular Biology* **215**: 403–410. https://doi.org/10.1016/S0022-2836(05)80360-2

Andersen SB, Geritsma S, Yusah KM, *et al.* (2009). The life of a dead ant: The expression of an adaptive extended phenotype. *The American Naturalist* **174**: 424–433. https://doi.org/10.1086/603640

Andriolli FS, Ishikawa NK, Vargas-Isla R, *et al.* (2019). Do zombie ant fungi turn their hosts into light seekers? *Behavioral Ecology* **30**:

609–616. https://doi.org/10.1093/beheco/ary198

AntWeb (2023). Version 8.87. California Academy of Science. https://www.antweb.org

AntWiki (2023). https://www.antwiki.org/wiki/Welcome_to_AntWiki

Araújo JPM, Evans HC, Geiser DM, *et al.* (2015). Unravelling the diversity behind the *Ophiocordyceps unilateralis* (*Ophiocordycipitaceae*) complex: Three new species of zombie-ant fungi from Brazilian Amazon. *Phytotaxa* **220**: 224–238. https://doi.org/10.11646/phytotaxa.220.3.2

Araújo JPM, Evans HC, Kepler R, *et al.* (2018). Zombie-ant fungi across continents: 15 new species and new combinations within *Ophiocordyceps*. I. Myrmecophilous hirsutelloid species. *Studies in Mycology* **90**: 119–160. https://doi.org/10.1016/j.simyco.2017.12.002

Araújo JPM, Evans HC, Fernandes IO, *et al.* (2020). Zombie-ant fungi cross continents: II. Myrmecophilous hymenostilboid species and a novel zombie lineage. *Mycologia* **112**: 1138–1170. https://doi.org/10.1080/00275514.2020.1822093

Araújo JPM, Hughes DP (2016). Diversity of entomopathogenic fungi: Which groups conquered the insect body? In: *Advances in Genetics: Genetics and molecular biology of entomopathogenic fungi* (Lovett B, Leger RJ eds). Elsevier, USA: 1–40. https://doi.org/10.1016/bs.adgen.2016.01.001

Araújo JPM, Hughes DP (2017). The fungal spore: Myrmecophilous *Ophiocordyceps* as a case study. In: *The fungal community: Its organization and role in the ecosystem* (Dighton J, White JF eds). CRC Press, USA: 359–367. https://doi.org/10.1201/9781315119496

Beckerson WC, Krider C, Mohammad UA, *et al.* (2023). 28 minutes later: investigating the role of aflatrem-like compounds in *Ophiocordyceps* parasite manipulation of zombie ants. *Animal Behaviour* **203**: 225–240. https://doi.org/10.1016/j.anbehav.2023.06.011

Bolton B (2024). An online catalogue of the ants of the world. https://antcat.org

Brecko J, Mathys A, Dekoninck W, *et al.* (2014). Focus stacking: Comparing commercial top-end set-ups with a semi-automatic low budget approach. A possible solution for mass digitization of type specimens. *ZooKeys* **464**: 1–23. https://doi.org/10.3897/zookeys.464.8615

Cardoso JA, Leal LC, Baccaro FB (2019). Temporal and spatial gradients of humidity shape the occurrence and the behavioral manipulation of ants infected by entomopathogenic fungi in Central Amazon. *Fungal Ecology* **42**: 1–10. https://doi.org/10.1016/j.funeco.2019.100871

Castlebury LA, Rossman AY, Sung G-H, *et al.* (2004). Multigene phylogeny reveals new lineage for *Stachybotrys chartarum*, the indoor air fungus. *Mycological Research* **108**: 864–872. https://doi.org/10.1017/S0953756204000607

CONANP (2023) *Estudio previo justificativo para el es*table*cimiento del área natural protegida Reserva de la Biosfera Sierra de Vallejo-Río Ameca, en los estados de Jalisco y Nayarit*. CONANP, México: 1–424. https://www.conanp.gob.mx/pdf/separata/EPJ-RB-SierraDeVallejo-RioAmeca.pdf

Creighton WS (1967). Living doors. *Natural History* **76**: 71–73.

Crous PW, Wingfield MJ, Burgess TI, *et al.* (2016). Fungal Planet description sheets: 469–557. *Persoonia* **37**: 218–403. https://doi.org/10.3767/003158516X694499

Dawkins WG (1982). *The extended phenotype*. Oxford University Press, England.

de Andrade CFS (1980). Epizootia natural causada por *Cordyceps unilateralis* (*Hypocreales*, *Euascomycetes*) em adultos de *Camponotus* sp. (*Hymenoptera*, *Formicidae*) na região de Manaus, Amazonas, Brasil. *Acta Amazonica* **10**: 671–677. https://doi.org/10.1590/1809-43921980103671

de Andrade ML, Baroni Urbani C (1999). Diversity and adaptation in the ant genus *Cephalotes*, past and present (*Hymenoptera*, *Formicidae*). *Stuttgarter Beiträge zur Naturkunde. Serie B (Geologie und Paläontologie)* **271**: 1–889.

de Bekker C, Quevillon LE, Smith PB, *et al.* (2014). Species-specific ant brain manipulation by a specialized fungal parasite. *BMC Evolutionary Biology* **14**: 1–12. https://doi.org/10.1186/s12862-014-0166-3

de Bekker C, Ohm RA, Loreto RG, *et al.* (2015). Gene expression during zombie ant biting behavior reflects the complexity underlying fungal parasitic behavioral manipulation. *BMC Genomics* **16**: 1–23. https://doi.org/10.1186/s12864-015-1812-x

de Bekker C, Ohm RA, Evans HC, *et al.* (2017). Ant-infecting *Ophiocordyceps* genomes reveal a high diversity of potential behavioral manipulation genes and a possible major role for enterotoxins. *Scientific Reports (Nature)* **7**: 12508. https://doi.org/10.1038/s41598-017-12863-w

Edgar RC (2004). MUSCLE: A multiple sequence alignment method with reduced time and space complexity. *BMC Bioinformatics* **5**: 113. https://doi.org/10.1186/1471-2105-5-113

Evans HC, Araújo JP, Halfeld VR, *et al.* (2018). Epitypification and re-description of the zombie-ant fungus, *Ophiocordyceps unilateralis* (*Ophiocordycipitaceae*). *Fungal Systematics and Evolution* **1**: 13–22. https://doi.org/10.3114/fuse.2018.01.02

Evans HC, Elliot SL, Hughes DP (2011a). Hidden diversity behind the zombie ant fungus *Ophiocordyceps unilateralis*: Four new species described from carpenter ants in Minas Gerais, Brazil. *PLoS ONE* **6**: e17024. https://doi.org/10.1371/journal.pone.0017024

Evans HC, Elliot SL, Hughes DP (2011b). *Ophiocordyceps unilateralis*: A keystone species for unraveling ecosystem functioning and biodiversity of fungi in tropical forest? *Communicative & Interrogative Biology* **4**: 598–602. https://doi.org/10.4161/cib.16721

Evans HC, Samson RA (1982). *Cordyceps* species and their anamorphs pathogenic on ants (*Formicidae*) in tropical forest ecosystems I. The *Cephalotes* (*Myrmicinae*) complex. *Transactions of the British Mycological Society* **79**: 431–453. https://doi.org/10.1016/S0007-1536(82)80037-5

Evans HC, Samson RA (1984). *Cordyceps* species and their anamorphs pathogenic on ants (*Formicidae*) in tropical forest ecosystems, II. The *Camponotus* (*Formicinae*) complex. *Transactions of the British Mycological Society* **82**: 127–150. https://doi.org/10.1016/S0007-1536(84)80219-3

Gordon DM (2012). The dynamics of foraging trails in the tropical arboreal ant *Cephalotes goniodontus*. *PLoS ONE* **7**: e50472. https://doi.org/10.1371/journal.pone.0050472

Guénard B, Weiser M, Gomez K, *et al.* (2017). The Global Ant Biodiversity Informatics (GABI) database: A synthesis of ant species geographic distributions. *Myrmecological News* **24**: 83–89. https://oist.repo.nii.ac.jp/record/196/files/mn24_83-89_printable.pdf

Guzmán G, Morón MA, Ramírez-Guillén F (2001). Entomogenous *Cordyceps* and related genera from Mexico with discussions on their hosts and new records. *Mycotaxon* **78**: 115–125. https://www.cabidigitallibrary.org/doi/full/10.5555/20013087944

Hadley A (2010). Combine ZP. https://combinezp.software.informer.com/download/

Hölldobler B, Wilson EO (1990). *The ants*. Harvard University Press,

USA.

Hywel-Jones NL (2002). The importance of invertebrate-pathogenic fungi from the tropics. In: *Tropical mycology: volume 2, micromycetes* (Watling R, Frankland JC, Ainsworth AM, *et al.* eds) CABI Publishing, England, UK: 133–144. https://doi.org/10.1079/9780851995434.0133

Imirzian N, Araújo JPM, Hughes DP (2020). A new zombie ant behavior unraveled: Aggregating on tree trunks. *Journal of Invertebrate Pathology* **177**: 107499. https://doi.org/10.1016/j.jip.2020.107499

Janicki J, Narula N, Ziegler M, *et al.* (2016). Visualizing and interacting with large-volume biodiversity data using client-server web-mapping applications: The design and implementation of antmaps.org. *Ecological Informatics* **32**: 185–193. https://doi.org/10.1016/j.ecoinf.2016.02.006

Kepler RM, Kaitsu Y, Tanaka E, *et al.* (2011) *Ophiocordyceps pulvinata sp. nov*., a pathogen of ants with a reduced stroma. *Mycoscience* **52**: 39–47. https://doi.org/10.1007/s10267-010-0072-5

Kobayasi Y (1941) The genus *Cordyceps* and its allies. *Science Reports* **5**: 53–260.

Kobmoo N, Mongkolsamrit S, Arnamnart N, *et al.* (2019). Population genomics revealed cryptic species within host-specific zombie-ant fungi (*Ophiocordyceps unilateralis*). *Molecular Phylogenetics and Evolution* **140**: 106580. https://doi.org/10.1016/j.ympev.2019.106580

Kobmoo N, Mongkolsamrit S, Wutikhun T, *et al.* (2012). Molecular phylogenies reveal host specific divergence of *Ophiocordyceps unilateralis* sensu lato following its host ants. *Molecular Ecology* **21**: 3022–3031. https://doi.org/10.1111/j.1365-294X.2012.05574.x

Kobmoo N, Mongkolsamrit S, Wutikhun T, *et al.* (2015). New species of *Ophiocordyceps unilateralis*, an ubiquitous pathogen of ants from Thailand. *Fungal Biology* **119**: 44–52. https://doi.org/10.1016/j.funbio.2014.10.008

Lavery MN, Murphy CFH, Bowman EK (2021). Zombie ant graveyard dynamics in Gunung Mulu National Park. *Reinvention: An International Journal of Undergraduate Research* **14**: https://doi.org/10.31273/reinvention.v14i1

Leaché AD, Reeder TW (2002). Molecular systematics of the eastern fence lizard (*Sceloporus undulatus*): A comparison of parsimony, likelihood, and Bayesian approaches. *Systematic Biology* **51**: 44–68. https://doi.org/10.1080/106351502753475871

Lin WJ, Lee YI, Liu SL, *et al.* (2020). Evaluating the trade-offs of a generalist parasitoid fungus, *Ophiocordyceps unilateralis*, on different sympatric ant hosts. *Scientific Reports* **10**: 1–12. https://doi.org/10.1038/s41598-020-63400-1

Liu YJ, Whelen S, Hall BD (1999). Phylogenetic relationships among ascomycetes: evidence from an RNA polymerse II subunit. *Molecular Biology and Evolution* **16**: 1799–1808. https://doi.org/10.1093/oxfordjournals.molbev.a026092

López-Rodríguez L, Burrola-Aguilar C, Sanjuan T (2023). *Cordyceps* sensu lato: the current state of knowledge in Mexico. *Scientia Fungorum* **54**: 1–24. https://doi.org/10.33885/sf.2023.54.1421

Loreto RG, Araújo JPM, Kepler RM, *et al.* (2018). Evidence for convergent evolution of host parasitic manipulation in response to environmental conditions. *Evolution* **72**: 2144–2155. https://doi.org/10.1111/evo.13489

Loreto RG, Elliot SL, Freitas ML, *et al.* (2014). Long-term disease dynamics for a specialized parasite of ant societies: A field study. *PLoS ONE* **9**: e103516. https://doi.org/10.1371/journal.pone.0103516

Lu Y, Tang D, Liu Z, *et al.* (2024). Genomic comparative analysis of *Ophiocordyceps unilateralis* sensu lato. *Frontiers in Microbiology* **15**: 1293077. https://doi.org/10.3389/fmicb.2024.1293077

Luangsa-ard JJ, Ridkaew R, Tasanathai K, *et al.* (2011). *Ophiocordyceps halabalaensis*: A new species of *Ophiocordyceps* pathogenic to *Camponotus gigas* in Hala Bala Wildlife Sanctuary, Southern Thailand. *Fungal Biology* **115**: 608–614. https://doi.org/10.1016/j.funbio.2011.03.002

Mackay WP (2019). *New World carpenter ants of the hyperdiverse genus* Camponotus (Hymenoptera: Formicidae)*, vol. 1: Introduction, subgenera, species complexes, and subgenus* Camponotus. Lambert Academic Publishing, Germany.

Mackay WP, Mackay EE (1989). Clave de los géneros de hormigas en México (*Hymenoptera*: *Formicidae*). In: *Memorias del II Simposio Nacional de Insectos Sociales Oaxtepec, Morelos* (Mackay WP, Mackay E, Quiroz LN, *et al.* eds). Sociedad Mexicana de Entomología, Mexico: 1–82.

Mackay WP, Mackay EE (2018). *A revision of the New World cork-headed ants of the genus* Colobopsis. Lambert Academic Publishing, Germany.

Mains EB (1951). Entomogenous species of *Hirsutella*, *Tilachlidium* and *Synnematium*. *Mycologia* **43**: 691–718. https://doi.org/10.1080/00275514.1951.12024164

Mains EB (1958). North American entomogenous species of *Cordyceps*. *Mycologia* **50**: 169–222. https://doi.org/10.2307/3756193

Maneval WE (1936). Lacto-phenol preparations. *Stain Technology* **11**: 9–11.

Miller MA, Pfeiffer W, Schwartz T (2010) Creating the CIPRES Science Gateway for inference of large phylogenetic trees. In: Gateway Computing Environments Workshop (GCE 2010) (Miller MA, Pfeiffer W, Schwartz T, eds). IEEE, USA: 1–8. https://doi.org/10.1109/GCE.2010.5676129

Minter DW, Brady BL (1980). Mononematous species of *Hirsutella*. *Transactions of the British Mycological Society* **74**: 271–282. https://doi.org/10.1016/S0007-1536(80)80157-4

Mongkolsamrit S, Kobmoo N, Tasanathai K, *et al.* (2012). Life cycle, host range and temporal variation of *Ophiocordyceps unilateralis*/*Hirsutella formicarum* on Formicine ants. *Journal of Invertebrate Pathology* **111**: 217–224. https://doi.org/10.1016/j.jip.2012.08.007

Morrone JJ (2020). *The Mexican transition zone. A natural biogeographic laboratory to study biotic assembly*. Springer, Switzerland. https://doi.org/10.1007/978-3-030-47917-6

Müller J, Müller K, Neinhuis C, *et al.* (2005). PhyDE® v0.9971. http://www.phyde.de/

Palacio EE, Fernández F (2003). Claves para las subfamilias y géneros. In: *Introducción a las hormigas de la región neotropical Bogotá* (Fernández F, ed). Instituto de Investigación de Recursos Biológicos Alexander von Humboldt, Colombia: 233–260.

Patouillard N (1892). Une Clavariée entomogène. *Revue Mycologique* **14**: 67–70. https://doi.org/10.13140/2.1.2183.8401

Pergande T (1896). Mexican Formicidae. *Proceedings of the California Academy of Sciences* **5**: 858–896.

Petch T (1924). Studies in entomogenous fungi. *Transactions of the British Mycological Society* **10**: 28–45.

Petch T (1931). Notes on entomogenous fungi. *Transactions of the British Mycological Society* **16**: 55–75.

Petch T (1934). Notes on entomogenous fungi. *Transactions of the British Mycological Society* **19**: 161–194.

Pincebourde S, Woods HA (2012). Climate uncertainty on leaf surfaces: The biophysics of leaf microclimates and their

consequences for leaf-dwelling organisms. *Functional Ecology* **26**: 844–853. https://doi.org/10.1111/j.1365-2435.2012.02013.x

Pontoppidan MB, Himaman W, Hywel-Jones NL, *et al.* (2009). Graveyards on the move: The spatio-temporal distribution of dead *Ophiocordyceps*-infected ants. *PloS ONE* **4**: e4835. https://doi.org/10.1371/journal.pone.0004835

Powell S, Price SL, Kronauer DJ (2020). Trait evolution is reversible, repeatable, and decoupled in the soldier caste of turtle ants. *Proceedings of the National Academy of Sciences USA* **117**: 6608–6615. https://doi.org/10.1073/pnas.1913750117

Rambaut A (2018). FigTree, a graphical viewer of phylogenetic trees (Version 1.4.4). https://tree.bio.ed.ac.uk/software/figtree/

Rambaut A, Drummond AJ, Xie D, et al. (2018). Posterior summarization in Bayesian phylogenetics using Tracer 1.7. *Systematic Biology* **67**: 901–904. https://doi.org/10.1093/sysbio/syy032

Ronquist F, Teslenko M, Van Der Mark P, *et al.* (2012). MrBayes 3.2: Efficient Bayesian phylogenetic inference and model choice across a large model space. *Systematic Biology* **61**: 539–542. https://doi.org/10.1093/sysbio/sys029

Rzedowski J (2006). *Vegetación de México* (1ra ed. digital). Comisión Nacional para el Conocimiento y Uso de la Biodiversidad, México. https://www.biodiversidad.gob.mx/publicaciones/librosDig/pdf/VegetacionMx_Cont.pdf

Saccardo PA (1895). *Cordyceps*. *Sylloge Fungorum* omnium hucusque cognitorum **11**: 366. https://doi.org/10.5962/bhl.title.5371

Saltamachia SJ, Araújo JPM (2020). *Ophiocordyceps desmidiospora*, a basal lineage within the "zombie-ant fungi" clade. *Mycologia* **112**: 1171–1183. https://doi.org/10.1080/00275514.2020.1732147

Sanjuan T, Henao LG, Amat G (2001). Distribución espacial de *Cordyceps* spp. (*Ascomycotina*: *Clavicipitaceae*) y su impacto sobre las hormigas en selvas del piedemonte amazónico de Colombia. *Revista de Biología Tropical* **49**: 945–955. https://www.scielo.sa.cr/scielo.php?pid=S0034-77442001000300014&script=sci_arttext

Sanjuan T, Franco-Molano AE, Kepler RM, *et al.* (2015). Five new species of entomopathogenic fungi from the Amazon and evolution of neotropical *Ophiocordyceps*. *Fungal Biology* **119**: 901–916. https://doi.org/10.1016/j.funbio.2015.06.010

Sayers EW, Beck J, Bolton EE, *et al.* (2022). Database resources of the national center for biotechnology information. *Nucleic Acids Research* **50**: D20–D26. https://doi.org/10.1093/nar/gkab1112

Schroeter J (1894)[1908]. Die Pilze Schlesiens. *Kryptogamen-Flora von Schlesien* **3.2(3)**: 257–384.

Stamatakis A (2014). RAxML version 8: A tool for phylogenetic analysis and post-analysis of large phylogenies. *Bioinformatics* **30**: 1312–1313. https://doi.org/10.1093/bioinformatics/btu033

Steensma, DP (2001). "Congo" red: out of Africa? *Archives of Pathology & Laboratory Medicine* **125**: 250–252. https://doi.org/10.5858/2001-125-0250-CR

Sung GH, Hywel-Jones NL, Sung JM, *et al.* (2007). Phylogenetic classification of *Cordyceps* and the clavicipitaceous fungi. *Studies in Mycology* **57**: 5–59. https://doi.org/10.3114/sim.2007.57.01

Tang D, Xu Z, Wang Y, *et al.* (2023a). Multigene phylogeny and morphology reveal two novel zombie-ant fungi in *Ophiocordyceps* (*Ophiocordycipitaceae*, *Hypocreales*). *Mycological Progress* **22**: 1–22. http://doi.org/10.1007/s11557-023-01874-9

Tang D, Huang O, Zou W, *et al.* (2023b). Six new species of zombie-ant fungi from Yunnan in China. *IMA Fungus* **14**: 1–33. http://doi.org/10.1186/s43008-023-00114-9

Tang D, Zhao J, Lu Y, *et al.* (2023c). Morphology, phylogeny and host specificity of two new *Ophiocordyceps* species belonging to the "zombie-ant fungi" clade (*Ophiocordycipitaceae*, *Hypocreales*). *MycoKeys* **99**: 269–296. https://doi.org/10.3897/mycokeys.99.107565

Technelysium (1996). ChromasPro v2.1.10. https://technelysium.com.au/wp/

Tulasne LR, Tulasne C (1865). Selecta Fungorum Carpologia III. Imperial Press, France. https://doi.org/10.5962/bhl.title.50436

Towns J, Cockerill T, Dahan M, *et al.* (2014). XSEDE: Accelerating scientific discovery. *Computing in Science & Engineering* **16**: 62–74. https://doi.org/10.1109/MCSE.2014.80

Turland NJ, Wiersema JH, Barrie FR, *et al.* (2018). *International Code of Nomenclature for algae, fungi, and plants (Shenzhen Code) adopted by the Nineteenth International Botanical Congress Shenzhen, China*. Koeltz Scientific Books, Germany.

Vásquez-Bolaños M (2011). Lista de especies de hormigas (*Hymenoptera*: *Formicidae*) para México. *Dugesiana* **18**: 95–133.

Vásquez-Bolaños M (2015). Taxonomía de Formicidae (*Hymenoptera*) para México. *Métodos en Ecología y Sistemática* **10**: 1–53.

Vergara-Torres CA, Vásquez-Bolaños M, Corona-López AM, *et al.* (2016). Ant (Hymenoptera: Formicidae) diversity in the canopy of a tropical dry forest in Tepoztlán, Central Mexico. *Annals of the Entomological Society of America* **110**: 197–203. https://doi.org/10.1093/aesa/saw074

Wei DP, Wanasinghe DN, Hyde KD, *et al.* (2020). *Ophiocordyceps tianshanensis* sp. nov. on ants from Tianshan mountains, PR China. *Phytotaxa* **464**: 277–292. https://doi.org/10.11646/phytotaxa.464.4.2

Wheeler WM (1927). The physiognomy of insects. *The Quarterly Review of Biology* **2**: 1–36.

Wheeler WM (1931). The ant *Camponotus* (*Myrmepomis*) *sericeiventris* Guérin and its mimic. *Psyche* **38**: 86–98. https://doi.org/10.1155/1931/98237

White TJ, Bruns T, Lee S, *et al.* (1990). Amplification and direct sequencing of fungal ribosomal RNA genes for phylogenetics. In: *PCR protocols: A guide to methods and applications* (Innis MA, Gelfand DH, Sninsky JJ, *et al.* eds). Academic Press, USA: 315–322.

Will I, Linehan S, Jenkins DG, *et al.* (2022). Natural history and ecological effects on the establishment and fate of Florida carpenter ant cadavers infected by the parasitic manipulator *Ophiocordyceps camponoti-floridani*. *Functional Ecology* **37**: 886–899. http://doi.org/10.1101/2022.10.21.513256

SUPPLEMENTARY MATERIAL

Table S1. Dataset of the type specimens sampled of the *Ophiocordyceps unilateralis* complex in western Mexico.

Table S2. Dataset of the hosts of the *Ophiocordyceps unilateralis* complex in western Mexico indicating *COI* sequences, entomological collection and locality data.